Frontiers of Information Technology & Electronic Engineering
www.zju.edu.cn/jzus; engineering.cae.cn; www.springerlink.com
ISSN 2095-9184 (print); ISSN 2095-9230 (online)
E-mail: jzus@zju.edu.cn

Adaptive robust beamformer for multi-pair two-way relay networks with imperfect channel state information*

Jin WANG[1], Feng SHU[†‡1,2,3], Ri-qing CHEN[2], Yu-di CUI[1], Yu CHEN[1], Jun LI[1]

([1]*School of Electronic and Optical Engineering, Nanjing University of Science and Technology, Nanjing 210094, China*)

([2]*College of Computer and Information Sciences, Fujian Agriculture and Forestry University, Fuzhou 350002, China*)

([3]*National Mobile Communications Research Laboratory, Southeast University, Nanjing 210096, China*)

[†]E-mail: shufeng@njust.edu.cn

Received Apr. 28, 2015; Revision accepted Dec. 7, 2015; Crosschecked Jan. 28, 2016

Abstract: In wideband multi-pair two-way relay networks, the performance of beamforming at a relay station (RS) is intimately related to the accuracy of the channel state information (CSI) available. The accuracy of CSI is determined by Doppler spread, delay between beamforming and channel estimation, and density of pilot symbols, including transmit power of pilot symbols. The coefficient of the Gaussian-Markov CSI error model is modeled as a function of CSI delay, Doppler spread, and signal-to-noise ratio, and can be estimated in real time. In accordance with the real-time estimated coefficients of the error model, an adaptive robust maximum signal-to-interference-and-noise ratio (Max-SINR) plus maximum signal-to-leakage-and-noise ratio (Max-SLNR) beamformer at an RS is proposed to track the variation of the CSI error. From simulation results and analysis, it is shown that: compared to existing non-adaptive beamformers, the proposed adaptive beamformer is more robust and performs much better in the sense of bit error rate (BER); with increase in the density of transmit pilot symbols, its BER and sum-rate performances tend to those of the beamformer of Max-SINR plus Max-SLNR with ideal CSI.

Key words: Multi-pair two-way relay, Adaptive robust beamformer, Channel state information (CSI), Maximum signal-to-interference-and-noise ratio (Max-SINR), Maximum signal-to-leakage-and-noise ratio (Max-SLNR)

http://dx.doi.org/10.1631/FITEE.1500134 **CLC number:** TN929.5

1 Introduction

Compared to one-way relay (Cover and Gamal, 1979; Laneman and Wornell, 2003; Sendonaris *et al.*, 2003; Kramer *et al.*, 2005; Zheng *et al.*, 2006; Zhong *et al.*, 2013) and single-pair two-way relay networks (Popovski and Yomo, 2006; Knopp, 2007; Rankov and Wittneben, 2007; Zhang *et al.*, 2009), multi-pair two-way relay systems have the following benefits: enhanced spectral efficiency/spatial multiplexing gain, multi-user diversity, and wider application fields (Yilmaz *et al.*, 2010; Degenhardt and Klein, 2012; Chen *et al.*, 2014; Shu *et al.*, 2014a; 2014b). Thus, it has become one of the most significant research topics in wireless communications and attracts a lot of attention from both industry and academia. In Yilmaz *et al.* (2010), zero-forcing (ZF) and block diagonalization (BD) were designed for multi-pair two-way relay networks with an amplify-and-forward (AF) strategy

‡ Corresponding author

* Project supported by the Open Research Fund of National Mobile Communications Research Laboratory, Southeast University, China (No. 2013D02), the Open Research Fund of National Key Laboratory of Electromagnetic Environment, China Research Institute of Radiowave Propagation (No. 201500013), the National Natural Science Foundation of China (Nos. 61271230, 61472190, and 61501238), the Research Fund for the Doctoral Program of Higher Education of China (No. 20113219120019), and the Jiangsu Provincial Science Foundation Project, China (No. BK20150786)

ORCID: Feng SHU, http://orcid.org/0000-0003-0073-1965

and analogy network coding is also developed under a quantize-and-forward (QF) strategy. Three multi-group multicast beamforming schemes including ZF, multicast-aware ZF, and signal-to-interference-and-noise ratio (SINR) balancing with bisection search were investigated in relay networks with a decode-and-forward (DF) strategy in Degenhardt and Klein (2012). In Shu *et al.* (2014b), two high-performance beamformers at a relay station (RS) were proposed and shown to be much better than ZF and BD in Yilmaz *et al.* (2010) in terms of sum-rate. Chen *et al.* (2014) proposed a high-performance maximum SINR (Max-SINR) plus maximum signal-to-leakage-and-noise ratio (Max-SLNR) beamformer per user at an RS, which was shown to perform better than the Max-SINR plus Max-SLNR per antenna in Shu *et al.* (2014b) in the sense of sum-rate. In Shu *et al.* (2014a), a spatial channel pairing (SCP) based on maximizing sum-rate (MSR) was proposed for AF-based multi-pair two-way relay networks. Additionally, a new mathematical inequality was proved and applied to derive the closed-form solution of the proposed SCP-MSR.

In the papers mentioned above, channel state information (CSI) at an RS was usually assumed to be perfect (Cover and Gamal, 1979; Laneman and Wornell, 2003). However, in practical systems, CSI can be obtained either through reverse channel estimation in time-division-duplex (TDD) by using the reciprocity between uplink and downlink or feedback in frequency-division-duplex (FDD) operation. Channel estimation usually generates errors. In conventional multi-user multi-input multi-output (MIMO) systems, a ZF precoder with imperfect CSI was proposed and its sum-rate expression was given and discussed (Mao *et al.*, 2012). Wang *et al.* (2007) investigated the impact of channel estimation error on bit error rate (BER) when the ZF precoder is adopted at the base station (BS), and proved an approximate distribution of signal-to-noise ratio (SNR) at the receiver. In Sadek *et al.* (2007), the conventional Max-SLNR precoder was redesigned by considering imperfect CSI. In one-way and two-way relay systems, robust beamforming at an RS was investigated (Chalise and Vandendorpe, 2009; Wang *et al.*, 2012; Shen *et al.*, 2013; Aziz *et al.*, 2014). Compared to a one-way relay, in a two-way relay scenario, elimination of self-interference at the mobile station is required. As a result, the channel estimation error has a more serious effect on a two-way system (Chalise and Vandendorpe, 2009; Shen *et al.*, 2013). In Wang *et al.* (2012), a closed-form formula of BER and an approximate formula of outage probability were derived with residual self-interference in a distributed two-way relay system. A beamforming method of minimizing the worst-case relay power under worst-case SINR constraints was designed for single-pair two-way relay systems in the presence of channel estimation errors (Aziz *et al.*, 2014).

To the best of our knowledge, almost all literature on robust beamforming at an RS or a BS makes the assumption that the variance or covariance matrix of the channel estimation error is fixed. However, in an actual wireless channel, due to the effect of time-variant fading and interference, the variance or covariance matrix of CSI from channel estimation usually varies with time and is not fixed. Therefore, in this paper, we develop an adaptive robust Max-SINR plus Max-SLNR beamformer of tracking the channel variation by taking Doppler spread, delay between channel estimation and beamforming, and the density and power of pilot symbols into account.

2 System model

Notations: throughout the paper, matrices, vectors, and scalars are denoted by letters of bold upper case, bold lower case, and lower case, respectively. Signs $(\cdot)^*$ and $(\cdot)^{\mathrm{H}}$ denote matrix conjugate and conjugate transpose, respectively. $\boldsymbol{I}_n$ denotes an $n \times n$ identity matrix.

A wideband multi-pair two-way relaying orthogonal frequency division multiplexing (OFDM) system is considered in this paper, where the total number of subcarriers is N_{C}, the length of cyclic prefix (CP) is L, and there is one central relay station (RS) and K pairs of multi-antenna mobile stations (MSs). The RS is equipped with N antennas and each MS has M antennas. All MSs exchange their information via the central RS during two time slots. Below, the two MSs of the kth user pair are denoted as k_a and k_b and we use $k_{(-i)}$ to denote the complement of k_i, $i \in S_{ab} = \{a, b\}$. In the second time slot, the received frequency-domain symbol at user k_i from user $k_{(-i)}$ corresponding to the qth subcarrier of the

uth OFDM symbol is

$$\begin{aligned}\boldsymbol{r}_{k_i}^{uq} =&\beta\left(\boldsymbol{G}_{k_i}^{uq}\right)^{\mathrm{T}}\boldsymbol{W}_{\mathrm{RS}}^{uq}\boldsymbol{H}_{k_{(-i)}}^{uq}\boldsymbol{s}_{k_{(-i)}}^{uq}\\&+\beta\left(\boldsymbol{G}_{k_i}^{uq}\right)^{\mathrm{T}}\boldsymbol{W}_{\mathrm{RS}}^{uq}\boldsymbol{H}_{k_i}^{uq}\boldsymbol{s}_{k_i}^{uq}+\boldsymbol{c}_{k_i}^{uq}\\&+\beta\left(\boldsymbol{G}_{k_i}^{uq}\right)^{\mathrm{T}}\boldsymbol{W}_{\mathrm{RS}}^{uq}\boldsymbol{z}_{\mathrm{RS}}^{uq}+\boldsymbol{z}_{k_i}^{uq},\end{aligned}\tag{1}$$

where $\boldsymbol{s}_{k_{(-i)}}^{uq}$ denotes the transmit symbol from user $k_{(-i)}$ to user k_i corresponding to the qth subcarrier of the uth OFDM symbol, $(\boldsymbol{G}_{k_i}^{uq})^{\mathrm{T}}$ and $\boldsymbol{H}_{k_i}^{uq}$ stand for the downlink and uplink channel matrices of user k_i corresponding to the qth subcarrier of the uth OFDM symbol respectively, $\boldsymbol{z}_{\mathrm{RS}}^{uq}$ and $\boldsymbol{z}_{k_i}^{uq}$ denote the additive white Gaussian noise (AWGN) vectors at the RS and user k_i respectively, and β is the normalized factor defined as

$$\begin{aligned}\beta =&P_{\mathrm{RS}}^{\frac{1}{2}}\Bigg\{\mathrm{tr}\sum_{m=1}^{M}\sum_{q=1}^{N_{\mathrm{C}}}\Bigg[\Big(\sum_{k=1}^{K}\sum_{i\in\{a,b\}}P_{\mathrm{MS}}M^{-1}\\&\cdot\boldsymbol{H}_{k_i}^{uq}\left(\boldsymbol{H}_{k_i}^{uq}\right)^{\mathrm{H}}+\sigma_{\mathrm{RS}}^2\boldsymbol{I}_N\Big)\left(\boldsymbol{W}_{\mathrm{RS}}^{uq}\right)^{\mathrm{H}}\boldsymbol{W}_{\mathrm{RS}}^{uq}\Bigg]\Bigg\}^{-\frac{1}{2}}\end{aligned}\tag{2}$$

at the RS and is designed such that the total transmit power at the RS is less than or equal to P_{RS}, where σ_{RS}^2 is the element-wise variance of the noise vector at the RS. In Eq. (1), $\boldsymbol{c}_{k_i}^{uq}$ is the total residual interference vector from other user pairs, defined as

$$\boldsymbol{c}_{k_i}^{uq}=\beta\left(\boldsymbol{G}_{k_i}^{uq}\right)^{\mathrm{T}}\boldsymbol{W}_{\mathrm{RS}}^{uq}\sum_{k'=1,k'\neq k}^{K}\sum_{i'\in\{a,b\}}\boldsymbol{H}_{k'_{i'}}^{uq}\boldsymbol{s}_{k'_{i'}}^{uq},\tag{3}$$

and $\boldsymbol{W}_{\mathrm{RS}}^{uq}$ represents the combined effect of the receive beamforming ($\boldsymbol{W}_{\mathrm{r},k_{(-i)}}^{uq}$) and transmit beamforming ($\boldsymbol{W}_{\mathrm{t},k_i}^{uq}$) at the RS corresponding to the qth subcarrier of the uth OFDM symbol, and is defined as

$$\boldsymbol{W}_{\mathrm{RS}}^{uq}=\sum_{k=1}^{K}\sum_{i\in\{a,b\}}\boldsymbol{W}_{\mathrm{t},k_i}^{uq}\left(\boldsymbol{W}_{\mathrm{r},k_{(-i)}}^{uq}\right)^{\mathrm{T}}.\tag{4}$$

The second term on the right-hand side of Eq. (1) is the self-interference signal, which can be completely cancelled at the MS, provided that the perfect CSI is available to MS k_i.

In a practical system, only imperfect CSI is available at an RS, and the CSI obtained by channel estimation will be affected by several factors such as the channel estimation error and time-varying properties of the wireless channel. Considering the uncertainty in CSI, similar to Zhou *et al.* (2011), the estimated channel matrices for beamforming at the RS are modeled as

$$\widehat{\boldsymbol{H}}_{k_i}^{(u-\Delta u)q}=\rho_{\mathrm{H}}\boldsymbol{H}_{k_i}^{uq}+\sqrt{1-\rho_{\mathrm{H}}^2}\boldsymbol{H}_{\mathrm{e},k_i}^{uq}\tag{5}$$

and

$$\widehat{\boldsymbol{G}}_{k_i}^{(u-\Delta u)q}=\rho_{\mathrm{G}}\boldsymbol{G}_{k_i}^{uq}+\sqrt{1-\rho_{\mathrm{G}}^2}\boldsymbol{G}_{\mathrm{e},k_i}^{uq},\tag{6}$$

where Δu is the corresponding delayed number of OFDM symbols between channel estimation and beamforming at the RS, and ρ_{H} and ρ_{G} are the error model coefficients for uplink and downlink channels, respectively. In the model above, $\widehat{\boldsymbol{H}}_{k_i}^{(u-\Delta u)q}$ and $\widehat{\boldsymbol{G}}_{k_i}^{(u-\Delta u)q}$ are the imperfect estimated channel matrices at the qth subcarrier of the uth symbol of user k_i, whereas $\boldsymbol{H}_{\mathrm{e},k_i}^{uq}$ and $\boldsymbol{G}_{\mathrm{e},k_i}^{uq}$ represent the error matrices from channel estimation and time-varying of the channel, whose entries are assumed to have independent identically distributed (i.i.d.) complex Gaussian random variables with variance σ_{H}^2 and σ_{G}^2, respectively. The remaining channel matrices $\boldsymbol{H}^{uq}$ and $\boldsymbol{G}^{uq}$ are the actual ideal channel matrices for beamforming at the time constant of beamforming at the RS. In general, they are unknown and are required to be anticipated by the model above and the known $\widehat{\boldsymbol{H}}_{k_i}^{(u-\Delta u)q}$ and $\widehat{\boldsymbol{G}}_{k_i}^{(u-\Delta u)q}$. However, two major factors contributing to the CSI error should be taken into account: (1) channel estimation error determined by the density of pilot symbols and the transmit power of the pilot; (2) time-varying error due to the time delay between channel estimation and beamforming at the RS and the Doppler spread. Due to the Doppler spread and channel fading, ρ_{H} and ρ_{G} in the model above should not be fixed. Hence, the constant models in Eqs. (5) and (6) are changed to the time-variant models:

$$\widehat{\boldsymbol{H}}_{k_i}^{(u-\Delta u)q}=\rho_{\mathrm{H},k_i}^{u}\boldsymbol{H}_{k_i}^{uq}+\xi_{\mathrm{H},k_i}^{u}\boldsymbol{H}_{\mathrm{e},k_i}^{uq}\tag{7}$$

and

$$\widehat{\boldsymbol{G}}_{k_i}^{(u-\Delta u)q}=\rho_{\mathrm{G},k_i}^{u}\boldsymbol{G}_{k_i}^{uq}+\xi_{\mathrm{G},k_i}^{u}\boldsymbol{G}_{\mathrm{e},k_i}^{uq},\tag{8}$$

where $\rho_{\mathrm{H},k_i}^{u}$ and $\rho_{\mathrm{G},k_i}^{u}$ are the time-variant error model coefficients, and the corresponding $\xi_{\mathrm{H},k_i}^{u}\triangleq\sqrt{1-\left(\rho_{\mathrm{H},k_i}^{u}\right)^2}$ and $\xi_{\mathrm{G},k_i}^{u}\triangleq\sqrt{1-\left(\rho_{\mathrm{G},k_i}^{u}\right)^2}$ measure the accuracy of CSI imperfection. $\rho_{\mathrm{H},k_i}^{u}$ and $\rho_{\mathrm{G},k_i}^{u}$ change from user to user, and from block to block. Here, one 'block' implies several frames or several hundred or even a thousand OFDM symbols.

Based on Eqs. (7) and (8), we design an adaptive method that the beamformer can follow and is robust against this variation. To simplify the estimation and derivation of ρ^u_{H,k_i} and ρ^u_{G,k_i} below, we suppose that pilot patterns for different users are designed to be orthogonal such that there is no interference among users in the training phase. Before beamforming at the RS, each user sends its own pilot symbols to the RS at the same time. For a wideband multi-pair two-way network, because of the time-domain properties of wireless channels, there are $2MKNL$ channel parameters that need to be estimated. In other words, each user will need at least ML pilot grids employed at the transmitter to complete a one-time channel estimation. This means at least ML distinct time-frequency grids are required at the transmitter. When the number of transmit time-frequency pilot grids is equal to ML, the received pilot frequency-domain symbol over subchannel q at the nth antenna of a BS from the mth transmit antenna of user k_i is equivalently written as

$$\tilde{Y}^{uq}_{k_i,mn} = H^{uq}_{k_i,mn}\tilde{s}^{uq}_{k_i,m} + \tilde{z}^{uq}_{k_i,mn}. \tag{9}$$

Then we can readily obtain the value of $G^{uq}_{k_i,mn}$ by making use of channel reciprocity between uplink and downlink. If the number of transmit time-frequency pilot grids is larger than $2M^2KL$, an SNR gain factor will be introduced to represent the increase in the number of pilot grids, as will be discussed later.

3 Proposed adaptive robust beamformer of Max-SINR plus Max-SLNR at a relay station

In this section, we design the transmit ($\boldsymbol{W}^{uq}_{\mathrm{t},k_i}$) and receive ($\boldsymbol{W}^{uq}_{\mathrm{r},k_{(-i)}}$) beamforming matrices at the RS by making use of Max-SINR and Max-SLNR criteria in the presence of imperfect CSI, respectively.

3.1 Proposed robust Max-SINR

In the first time slot, the receive signal vector in the absence of beamforming at the RS is

$$\boldsymbol{r}^{uq}_{\mathrm{RS}} = \boldsymbol{H}^{uq}_{k_i}\boldsymbol{s}^{uq}_{k_i} + \boldsymbol{H}^{uq}_{k_{(-i)}}\boldsymbol{s}^{uq}_{k_{(-i)}} + \boldsymbol{H}^{uq}_{-k}\boldsymbol{s}^{uq}_{-k} + \boldsymbol{z}^{uq}_{\mathrm{RS}}, \tag{10}$$

where $-k$ denotes the set $\{1_a, 1_b, 2_a, \ldots, (k-1)_b, (k+1)_a, (k+1)_b, \ldots, K_b\}$ and $\boldsymbol{H}^{uq}_{-k} = [\boldsymbol{H}^{uq}_{1_a}, \boldsymbol{H}^{uq}_{1_b}, \ldots, \boldsymbol{H}^{uq}_{(k-1)_b}, \boldsymbol{H}^{uq}_{(k+1)_a}, \boldsymbol{H}^{uq}_{(k+1)_b}, \ldots, \boldsymbol{H}^{uq}_{K_b}]$. The first-stage receive beamforming matrix $\left(\boldsymbol{W}^{uq}_{\mathrm{r},k_{(-i)}}\right)^{\mathrm{T}}$ at the RS is applied to the total receive signal vector $\boldsymbol{r}_{\mathrm{RS}}$ at the RS and forms a new signal for the link from user $k_{(-i)}$ to user k_i:

$$\begin{aligned}\boldsymbol{x}^{uq}_{\mathrm{RS},k_{(-i)}} = &\left(\boldsymbol{W}^{uq}_{\mathrm{r},k_{(-i)}}\right)^{\mathrm{T}}\boldsymbol{H}^{uq}_{k_i}\boldsymbol{s}^{uq}_{k_i}\\ &+\left(\boldsymbol{W}^{uq}_{\mathrm{r},k_{(-i)}}\right)^{\mathrm{T}}\boldsymbol{H}^{uq}_{k_{(-i)}}\boldsymbol{s}^{uq}_{k_{(-i)}}\\ &+\left(\boldsymbol{W}^{uq}_{\mathrm{r},k_{(-i)}}\right)^{\mathrm{T}}\boldsymbol{H}^{uq}_{-k}\boldsymbol{s}^{uq}_{-k} + \boldsymbol{z}^{uq}_{\mathrm{RS}},\end{aligned} \tag{11}$$

where $\boldsymbol{W}^{uq}_{\mathrm{r},k_{(-i)}}$ is obtained by maximizing the SINR of user $k_{(-i)}$ corresponding to the qth subcarrier of the uth OFDM symbol. Since the imperfect CSI is available at the RS, the self-interference cannot be cancelled completely. From Eqs. (7) and (11), given that $\widehat{\boldsymbol{H}}^{(u-\Delta u)q}_{k_i}$ and ρ^u_{H,k_i} are known or can be estimated, the average SINR of user $k_{(-i)}$ corresponding to the qth subcarrier of the uth OFDM symbol is formulated as

$$\begin{aligned}\mathrm{SINR}^{uq}_{k_{(-i)}} = &P_{\mathrm{MS}}M^{-1}\mathrm{tr}\left(\left(\boldsymbol{W}^{uq}_{\mathrm{r},k_{(-i)}}\right)^{\mathrm{T}}\boldsymbol{\Phi}_1\right.\\ &\left.\cdot\left(\boldsymbol{W}^{uq}_{\mathrm{r},k_{(-i)}}\right)^{*}\right)\cdot\left[\sigma^2_{\mathrm{RS}} + P_{\mathrm{MS}}M^{-1}\right.\\ &\left.\cdot\mathrm{tr}\left(\left(\boldsymbol{W}^{uq}_{\mathrm{r},k_{(-i)}}\right)^{\mathrm{T}}(\boldsymbol{\Phi}_2+\boldsymbol{\Phi}_3)\left(\boldsymbol{W}^{uq}_{\mathrm{r},k_{(-i)}}\right)^{*}\right)\right]^{-1},\end{aligned} \tag{12}$$

where $\boldsymbol{\Phi}_1$, $\boldsymbol{\Phi}_2$, and $\boldsymbol{\Phi}_3$ are the covariance matrices of channels corresponding to the useful signal, interference from other user pairs, and the residual interference signal due to imperfect CSI, respectively, defined as

$$\boldsymbol{\Phi}_1 = E\left[\boldsymbol{H}^{uq}_{k_{(-i)}}\left(\boldsymbol{H}^{uq}_{k_{(-i)}}\right)^{\mathrm{H}}\middle|\rho^u_{\mathrm{H},k_{(-i)}}, \widehat{\boldsymbol{H}}^{(u-\Delta u)q}_{k_{(-i)}}\right], \tag{13}$$

$$\begin{aligned}\boldsymbol{\Phi}_2 = E\Big[\boldsymbol{H}^{uq}_{-k}\left(\boldsymbol{H}^{uq}_{-k}\right)^{\mathrm{H}}\Big|\Big\{&\rho^u_{\mathrm{H},1_a}, \rho^u_{\mathrm{H},1_b}, \ldots, \rho^u_{\mathrm{H},(k-1)_b},\\ &\rho^u_{\mathrm{H},(k+1)_a}, \ldots, \rho^u_{\mathrm{H},K_a}, \rho^u_{\mathrm{H},K_b}\Big\}, \widehat{\boldsymbol{H}}^{(u-\Delta u)q}_{-k}\Big],\end{aligned} \tag{14}$$

$$\boldsymbol{\Phi}_3 = E\left[\boldsymbol{H}^{uq}_{\mathrm{e},k_i}\left(\boldsymbol{H}^{uq}_{\mathrm{e},k_i}\right)^{\mathrm{H}}\middle|\rho^u_{\mathrm{H},k_i}, \widehat{\boldsymbol{H}}^{(u-\Delta u)q}_{k_i}\right]. \tag{15}$$

The optimal receive beamforming matrix ($\boldsymbol{W}^{uq}_{\mathrm{r},k_{(-i)}}$) is obtained by maximizing the above

SINR corresponding to the qth subcarrier of the uth OFDM symbol of user $k_{(-i)}$ in Eq. (12), which is reduced to the eigenvector of the largest M eigenvalues of matrix $\boldsymbol{A}_{k_{(-i)}}$:

$$\boldsymbol{A}_{k_{(-i)}}=\frac{\boldsymbol{\Phi}_1^{\mathrm{T}}}{\sigma_{\mathrm{RS}}^2\boldsymbol{I}_N+P_{\mathrm{MS}}M^{-1}\left(\boldsymbol{\Phi}_2+\boldsymbol{\Phi}_3\right)^{\mathrm{T}}},\quad(16)$$

which, in accordance with the derivation in Appendix A, can be further simplified as Eq. (17) where σ_{MS}^2 is the element-wise variance of the noise vector at the MS. Obviously, if ρ_{H,k_i}^u in Eq. (17) can be estimated and updated periodically, the above robust receive beamformer becomes an adaptive one. This is also consistent with the real wireless scenario.

3.2 Proposed robust Max-SLNR

In the second time slot, the downlink channel is viewed as a broadcasting channel. Considering the duality between Max-SINR in uplink and Max-SLNR in downlink, Max-SLNR can be applied to the second time slot to further compress the interference from other user pairs. Provided that $\widehat{\boldsymbol{G}}_{k_i}^{(u-\Delta u)q}$ and ρ_{G,k_i}^u are known or can be estimated, using the concept of leakage, the average SLNR of the transmit signal of user k_i corresponding to the qth subcarrier of the uth OFDM symbol to other user pairs is defined as

$$\mathrm{SLNR}_{k_i}^{uq}=\frac{P_{\mathrm{RS}}N^{-1}\mathrm{tr}\left(\boldsymbol{W}_{\mathrm{t},k_i}^{uq}\boldsymbol{\Psi}_1\left(\boldsymbol{W}_{\mathrm{t},k_i}^{uq}\right)^{\mathrm{H}}\right)}{\sigma_{\mathrm{MS}}^2+P_{\mathrm{RS}}N^{-1}\mathrm{tr}\left(\boldsymbol{W}_{\mathrm{t},k_i}^{uq}\left(\boldsymbol{\Psi}_2+\boldsymbol{\Psi}_3\right)\left(\boldsymbol{W}_{\mathrm{t},k_i}^{uq}\right)^{\mathrm{H}}\right)},\quad(18)$$

where $\boldsymbol{\Psi}_1$, $\boldsymbol{\Psi}_2$, and $\boldsymbol{\Psi}_3$ are the transmit signal, the leakage signal to other user pairs, and the leakage interference from imperfect CSI, respectively:

$$\boldsymbol{\Psi}_1=E\left[\left(\boldsymbol{G}_{k_i}^{uq}\right)^*\left(\boldsymbol{G}_{k_i}^{uq}\right)^{\mathrm{T}}\middle|\rho_{\mathrm{G},k_i}^u,\widehat{\boldsymbol{G}}_{k_i}^{(u-\Delta u)q}\right],\quad(19)$$

$$\boldsymbol{\Psi}_2=E\left[\left(\boldsymbol{G}_{-k}^{uq}\right)^*\left(\boldsymbol{G}_{-k}^{uq}\right)^{\mathrm{T}}\middle|\left\{\rho_{\mathrm{G},1_a}^u,\rho_{\mathrm{G},1_b}^u,\ldots,\rho_{\mathrm{G},(k-1)_b}^u,\rho_{\mathrm{G},(k+1)_a}^u,\ldots,\rho_{\mathrm{G},K_a}^u,\rho_{\mathrm{G},K_b}^u\right\},\widehat{\boldsymbol{G}}_{-k}^{(u-\Delta u)q}\right],\quad(20)$$

$$\boldsymbol{\Psi}_3=E\left[\left(\boldsymbol{G}_{k_{(-i)}}^{uq}-\widehat{\boldsymbol{G}}_{k_{(-i)}}^{(u-\Delta u)q}\right)^*\cdot\left(\boldsymbol{G}_{k_{(-i)}}^{uq}-\widehat{\boldsymbol{G}}_{k_{(-i)}}^{(u-\Delta u)q}\right)^{\mathrm{T}}\middle|\rho_{\mathrm{G},k_{(-i)}}^u,\widehat{\boldsymbol{G}}_{k_{(-i)}}^{(u-\Delta u)q}\right].\quad(21)$$

In a similar way, the column vectors of the transmit beamforming matrix ($\boldsymbol{W}_{\mathrm{t},k_i}^{uq}$) consist of the

$$\begin{aligned}\boldsymbol{A}_{k_{(-i)}}=&\left\{\left(\frac{\sigma_{\mathrm{H}}^2\xi_{\mathrm{H},k_{(-i)}}^u}{\left(\xi_{\mathrm{H},k_{(-i)}}^u\right)^2\rho_{\mathrm{H},k_{(-i)}}^u\sigma_{\mathrm{H}}^2+\left(\rho_{\mathrm{H},k_{(-i)}}^u\right)^3}-\frac{1}{\rho_{\mathrm{H},k_{(-i)}}^u}\right)^2\left(\widehat{\boldsymbol{H}}_{k_{(-i)}}^{(u-\Delta u)q}\right)^*\left(\widehat{\boldsymbol{H}}_{k_{(-i)}}^{(u-\Delta u)q}\right)^{\mathrm{T}}\right.\\&\left.+\frac{N\sigma_{\mathrm{H}}^2\left(\xi_{\mathrm{H},k_{(-i)}}^u\right)^2}{\left(\xi_{\mathrm{H},k_{(-i)}}^u\right)^2\sigma_{\mathrm{H}}^2+\left(\rho_{\mathrm{H},k_{(-i)}}^u\right)^2}\boldsymbol{I}_N\right\}\left\{\sigma_{\mathrm{MS}}^2\boldsymbol{I}_N+\frac{P_{\mathrm{MS}}}{M}\left[\left(\frac{\sigma_{\mathrm{H}}^2\xi_{\mathrm{H},k_i}^u}{\left(\xi_{\mathrm{H},k_i}^u\right)^2\rho_{\mathrm{H},k_i}^u\sigma_{\mathrm{H}}^2+\left(\rho_{\mathrm{H},k_i}^u\right)^3}\right.\right.\right.\\&\left.-\frac{1-\rho_{\mathrm{H},k_i}^u}{\rho_{\mathrm{H},k_i}^u}\right)^2\left(\widehat{\boldsymbol{H}}_{k_i}^{(u-\Delta u)q}\right)^*\left(\widehat{\boldsymbol{H}}_{k_i}^{(u-\Delta u)q}\right)^{\mathrm{T}}+\frac{N\sigma_{\mathrm{H}}^2\left(\xi_{\mathrm{H},k_i}^u\right)^2}{\left(\xi_{\mathrm{H},k_i}^u\right)^2\sigma_{\mathrm{H}}^2+\left(\rho_{\mathrm{H},k_i}^u\right)^2}\boldsymbol{I}_N\\&+\sum_{k'=1,k'\neq k}^{K}\sum_{i'\in\{a,b\}}\left(\frac{\sigma_{\mathrm{H}}^2\xi_{\mathrm{H},k'_{i'}}^u}{\left(\xi_{\mathrm{H},k'_{i'}}^u\right)^2\rho_{\mathrm{H},k'_{i'}}^u\sigma_{\mathrm{H}}^2+\left(\rho_{\mathrm{H},k'_{i'}}^u\right)^3}-\frac{1}{\rho_{\mathrm{H},k'_{i'}}^u}\right)^2\left(\widehat{\boldsymbol{H}}_{k'_{i'}}^{(u-\Delta u)q}\right)^*\left(\widehat{\boldsymbol{H}}_{k'_{i'}}^{(u-\Delta u)q}\right)^{\mathrm{T}}\\&\left.\left.+\sum_{k'=1,k'\neq k}^{K}\sum_{i'\in\{a,b\}}\frac{N\sigma_{\mathrm{H}}^2\left(\xi_{\mathrm{H},k'_{i'}}^u\right)^2}{\left(\xi_{\mathrm{H},k'_{i'}}^u\right)^2\sigma_{\mathrm{H}}^2+\left(\rho_{\mathrm{H},k'_{i'}}^u\right)^2}\boldsymbol{I}_N\right]\right\}^{-1}.\end{aligned}\quad(17)$$

eigenvectors corresponding to the largest M eigenvalues of matrix $\boldsymbol{B}_{k_i}$:

$$\boldsymbol{B}_{k_i}=\frac{\boldsymbol{\Psi}_1}{\sigma_{\mathrm{RS}}^2\boldsymbol{I}_N+P_{\mathrm{RS}}N^{-1}\left(\boldsymbol{\Psi}_2+\boldsymbol{\Psi}_3\right)}, \tag{22}$$

which, in accordance with the derivation in Appendix B, can be further simplified as Eq. (23).

We have now completed the construction of a robust Max-SINR plus Max-SLNR beamformer at the RS. To make the proposed robust beamformer adaptive, we specify how to make a real-time estimation of the error model coefficients ρ_{H,k_i}^u and ρ_{G,k_i}^u in Eqs. (17) and (23), respectively, in the next section.

4 Real-time estimation of Markov-Gaussian error model coefficients

For the convenience of the following derivation, the error model coefficients ρ_{H,k_i}^u and ρ_{G,k_i}^u are decomposed into a product of two factors:

$$\rho_{\mathrm{H},k_i}^u=\rho_{\mathrm{H},k_i}^{u\mathrm{d}}\rho_{\mathrm{H},k_i}^{u\mathrm{e}}, \tag{24}$$

$$\rho_{\mathrm{G},k_i}^u=\rho_{\mathrm{G},k_i}^{u\mathrm{d}}\rho_{\mathrm{G},k_i}^{u\mathrm{e}}, \tag{25}$$

which are related to time variation in the channel and channel estimation error, respectively. In Eqs. (24) and (25), $\rho_{\mathrm{H},k_i}^{u\mathrm{d}}$ and $\rho_{\mathrm{G},k_i}^{u\mathrm{d}}$ measure the effect of channel mismatching on channels corresponding to slots one and two caused by the Doppler spread due to time delay between channel estimation and beamforming, respectively, whereas $\rho_{\mathrm{H},k_i}^{u\mathrm{e}}$ and $\rho_{\mathrm{G},k_i}^{u\mathrm{e}}$ measure the effect of channel mismatching on channels corresponding to slots one and two due to the estimation error, respectively. In the following subsections, $\rho_{\mathrm{H},k_i}^{u\mathrm{e}}$ and $\rho_{\mathrm{G},k_i}^{u\mathrm{e}}$ are modeled as functions of Doppler spread, CSI delay, and average SNR at pilot grids.

To realize the real-time estimation of ρ_{G,k_i}^u and ρ_{H,k_i}^u, we suppose that the RS broadcasts N_{p} continuous pilot OFDM symbols, with each having the same length and transmit power as data OFDM symbols, to all user pairs, and the frequency-domain pilot matrix associated with the uth pilot OFDM symbol is denoted as $\bar{\boldsymbol{X}}^u$ being an $N_{\mathrm{C}}\times N$ matrix with each column consisting of a pseudo-noise (PN) sequence. After these pilot OFDM symbols passing through the channel, the t samples of the received pilot time-domain OFDM symbol at the mth receive antenna of user k_i from the nth antenna of the RS are expressed as $\bar{y}_{k_i,mn}^u(t)$ where t varies from 0 to $N_{\mathrm{C}}+L-1$. Each user estimates its own SNR and Doppler spread by using the corresponding received OFDM symbol and feeds back these estimated values to the RS. In terms of these values, the RS computes all ρ_{G,k_i}^u and ρ_{H,k_i}^u and updates the beamforming matrix at the RS as shown in Eq. (1) in terms of Eqs. (4), (17), and (23).

$$\begin{aligned}\boldsymbol{B}_{k_i}=&\left\{\left(\frac{\sigma_{\mathrm{G}}^2\xi_{\mathrm{G},k_i}^u}{\left(\xi_{\mathrm{G},k_i}^u\right)^2\rho_{\mathrm{G},k_i}^u\sigma_{\mathrm{G}}^2+\left(\rho_{\mathrm{G},k_i}^u\right)^3}-\frac{1}{\rho_{\mathrm{G},k_i}^u}\right)^2\left(\widehat{\boldsymbol{G}}_{k_i}^{(u-\Delta u)q}\right)^*\left(\widehat{\boldsymbol{G}}_{k_i}^{(u-\Delta u)q}\right)^{\mathrm{T}}\right.\\&\left.+\frac{N\sigma_{\mathrm{G}}^2\left(\xi_{\mathrm{G},k_i}^u\right)^2}{\left(\xi_{\mathrm{G},k_i}^u\right)^2\sigma_{\mathrm{G}}^2+\left(\rho_{\mathrm{G},k_i}^u\right)^2}\boldsymbol{I}_N\right\}\left\{\sigma_{\mathrm{RS}}^2\boldsymbol{I}_N+\frac{P_{\mathrm{RS}}}{N}\left[\left(\frac{\sigma_{\mathrm{G}}^2\xi_{\mathrm{G},k_{(-i)}}^u}{\left(\xi_{\mathrm{G},k_{(-i)}}^u\right)^2\rho_{\mathrm{G},k_{(-i)}}^u\sigma_{\mathrm{G}}^2+\left(\rho_{\mathrm{G},k_{(-i)}}^u\right)^3}\right.\right.\right.\\&\left.-\frac{1-\rho_{\mathrm{G},k_{(-i)}}^u}{\rho_{\mathrm{G},k_{(-i)}}^u}\right)^2\left(\widehat{\boldsymbol{G}}_{k_{(-i)}}^{(u-\Delta u)q}\right)^*\left(\widehat{\boldsymbol{G}}_{k_{(-i)}}^{(u-\Delta u)q}\right)^{\mathrm{T}}+\frac{N\sigma_{\mathrm{H}}^2\left(\xi_{\mathrm{G},k_{(-i)}}^u\right)^2}{\left(\xi_{\mathrm{G},k_{(-i)}}^u\right)^2\sigma_{\mathrm{G}}^2+\left(\rho_{\mathrm{G},k_{(-i)}}^u\right)^2}\boldsymbol{I}_N\\&+\sum_{k'=1,k'\neq k}^{K}\sum_{i'\in\{a,b\}}\left(\frac{\sigma_{\mathrm{G}}^2\xi_{\mathrm{G},k'_{i'}}^u}{\left(\xi_{\mathrm{G},k'_{i'}}^u\right)^2\rho_{\mathrm{G},k'_{i'}}^u\sigma_{\mathrm{G}}^2+\left(\rho_{\mathrm{G},k'_{i'}}^u\right)^3}-\frac{1}{\rho_{\mathrm{G},k'_{i'}}^u}\right)^2\left(\widehat{\boldsymbol{G}}_{k'_{i'}}^{(u-\Delta u)q}\right)^*\left(\widehat{\boldsymbol{G}}_{k'_{i'}}^{(u-\Delta u)q}\right)^{\mathrm{T}}\\&\left.\left.+\sum_{k'=1,k'\neq k}^{K}\sum_{i'\in\{a,b\}}\frac{N\sigma_{\mathrm{G}}^2\left(\xi_{\mathrm{G},k'_{i'}}^u\right)^2}{\left(\xi_{\mathrm{G},k'_{i'}}^u\right)^2\sigma_{\mathrm{G}}^2+\left(\rho_{\mathrm{G},k'_{i'}}^u\right)^2}\boldsymbol{I}_N\right]\right\}^{-1}.\end{aligned} \tag{23}$$

4.1 Error parameter associated with Doppler spread

In this subsection, we show how to compute $\rho^{ud}_{\mathrm{H},k_i}$. Note that $\Delta u T_\mathrm{s}$ stands for the time delay between channel estimation and beamforming at the RS, where T_s is the total length of the OFDM symbols and Δu is the corresponding delayed number of the OFDM symbols. To simplify the derivation, we assume $\rho^{ue}_{\mathrm{H},k_i}=1$. $\rho^{ud}_{\mathrm{H},k_i}$ can be obtained using the minimum mean-square error (MMSE) criterion. The complex channel gain from the mth antenna of user k_i to the nth antenna of the RS at the qth subcarrier of the uth OFDM symbol is modeled as

$$\widehat{H}^{(u-\Delta u)q}_{k_i,mn}=\rho^{ud}_{\mathrm{H},k_i}H^{uq}_{k_i,mn}+\xi^{ud}_{\mathrm{H},k_i}H^{uq}_{\mathrm{e},k_i,mn}, \tag{26}$$

where the first term in the right-hand side of Eq. (26) denotes the ideal channel gain at the $(u-\Delta u)$th OFDM symbol and the second term is the error caused by the Δuth OFDM symbol delay.

Given that $\tilde{s}^{uq}_{k_i,m}$ is the pilot symbol transmitted by the transmitter and known at the receiver, substituting Eq. (26) into the following expression:

$$E\left(\left|\tilde{Y}^{uq}_{k_i,mn}-\widehat{H}^{uq}_{k_i,mn}\tilde{s}^{uq}_{k_i,m}\right|^2\right), \tag{27}$$

as shown in Appendix C, and minimizing the above mean square error (MSE) by taking the derivative of the above expression with respect to $\rho^{ud}_{\mathrm{H},k_i}$, will yield

$$\rho^{ud}_{\mathrm{H},k_i}=\frac{\Re_{\mathrm{HH},k_i}(\Delta u,0)}{\Re_{\mathrm{HH},k_i}(0,0)}, \tag{28}$$

where $\Re_{\mathrm{HH},k_i}(\Delta u,\Delta q)$ is the time-frequency channel correlation function defined by

$$\Re_{\mathrm{HH},k_i}(\Delta u,\Delta q)=E\left(H^{uq}_{k_i,mn}\left(H^{(u+\Delta u)(q+\Delta q)}_{k_i,mn}\right)^*\right). \tag{29}$$

In typical urban (TU) channels, $\Re_{\mathrm{HH},k_i}(\Delta u,0)$ in Eq. (28) can be written as

$$\Re_{\mathrm{HH},k_i}(\Delta u,0)=J_0\left(2\pi f^u_{\mathrm{d},k_i}\Delta u T_\mathrm{s}\right), \tag{30}$$

where function $J_0(\cdot)$ is the zeroth-order Bessel function of the first kind:

$$J_0(x)=\frac{1}{x}\int_0^\pi \mathrm{e}^{\mathrm{j}x\cos\theta}\mathrm{d}\theta, \tag{31}$$

and f^u_{d,k_i} is the Doppler spread of user k_i. In terms of Eq. (28), we can compute $\rho^{ud}_{\mathrm{H},k_i}$ under given f^u_{d,k_i}. By exploiting the cyclic property of CP of the OFDM symbol, the Doppler spread f^u_{d,k_i} is estimated as Eq. (32) (Holtzman and Sampath, 1995; Tepedelenlioglu and Giannakis, 2001; Baddour and Beaulieu, 2003):

$$\widehat{f^u_{\mathrm{d},k_i}}=\frac{1}{2\pi}\sqrt{\frac{-2r''_{yy}(0)}{r_{yy}(0)}}=\frac{1}{2\pi T_\mathrm{s}}\cdot\sqrt{\frac{4\sum\limits_{u=1}^{N_\mathrm{p}}\sum\limits_{m=1}^{M}\sum\limits_{n=1}^{N}\sum\limits_{t=0}^{L-1}\left(\left|\bar{y}^u_{k_i,mn}(t)\right|^2-\left|\bar{y}^u_{k_i,mn}(t+N_\mathrm{C})\right|^2\right)}{\sum\limits_{u=1}^{N_\mathrm{p}}\sum\limits_{m=1}^{M}\sum\limits_{n=1}^{N}\sum\limits_{t=0}^{L-1}\left(\left|\bar{y}^u_{k_i,mn}(t)\right|^2+\left|\bar{y}^u_{k_i,mn}(t+N_\mathrm{C})\right|^2\right)}}, \tag{32}$$

where $y^u_{k_i,mn}$ is the time-domain received signal from the mth antenna of user k_i to the nth antenna of the RS corresponding to the uth OFDM symbol. In a similar manner, we can estimate $\rho^{ud}_{\mathrm{G},k_i}$ readily.

4.2 Error parameter associated with channel estimation error

Now, we specify how to estimate parameter $\rho^{ue}_{\mathrm{H},k_i}$ associated with channel estimation. The accuracy of channel estimation relies directly upon the average SNR ($\mathrm{SNR}^{up}_{\mathrm{H},k_i}$) at pilot grids in the channel given an estimator like MMSE, while $\mathrm{SNR}^{up}_{\mathrm{H},k_i}$ is approximately proportional to the average SNR ($\mathrm{SNR}^{ud}_{\mathrm{H},k_i}$) at data grids. For simplicity, the estimation process of $\rho^{ue}_{\mathrm{H},k_i}$ is divided into three steps: (1) establish its relation to $\mathrm{SNR}^{up}_{\mathrm{H},k_i}$ given the channel estimator; (2) model $\mathrm{SNR}^{up}_{\mathrm{H},k_i}$ as a linear function of $\mathrm{SNR}^{ud}_{\mathrm{H},k_i}$; (3) estimate $\mathrm{SNR}^{ud}_{\mathrm{H},k_i}$ using the CP-based correlation method. In Appendix D, after the linear MMSE (LMMSE) channel estimator is adopted, parameter $\rho^{ue}_{\mathrm{H},k_i}$ is proved to be

$$\rho^{ue}_{\mathrm{H},k_i}=\frac{\mathrm{SNR}^{up}_{\mathrm{H},k_i}}{1+\mathrm{SNR}^{up}_{\mathrm{H},k_i}}. \tag{33}$$

Considering the transmit power of pilot symbols and the number of pilot symbols per channel parameter, we approximate $\mathrm{SNR}^{up}_{\mathrm{H},k_i}$ as a linear function of $\mathrm{SNR}^{ud}_{\mathrm{H},k_i}$ as follows:

$$\mathrm{SNR}^{up}_{\mathrm{H},k_i}\approx\alpha_{\mathrm{H},k_i}\mathrm{SNR}^{ud}_{\mathrm{H},k_i}, \tag{34}$$

where α_{H,k_i} is defined as

$$\alpha_{\mathrm{H},k_i}=\frac{P^\mathrm{p}_{\mathrm{H},k_i}}{P^\mathrm{d}_{\mathrm{H},k_i}}\frac{L^\mathrm{p}_{\mathrm{H},k_i}}{L^\mathrm{c}_{\mathrm{H},k_i}}, \tag{35}$$

where $P^{\mathrm{p}}_{\mathrm{H},k_i}$ and $L^{\mathrm{p}}_{\mathrm{H},k_i}$ are the average transmit power of pilot symbols and the total number of pilot symbols per estimation use, $P^{\mathrm{d}}_{\mathrm{H},k_i}$ is the average power of data symbols, and $L^{\mathrm{c}}_{\mathrm{H},k_i}$ denotes the number of channel parameters that need to be estimated. Due to the cyclic property of CP in the OFDM system, $\mathrm{SNR}^{ud}_{\mathrm{H},k_i}$ is estimated by the following expression:

$$\mathrm{SNR}^{ud}_{\mathrm{H},k_i} = \frac{\sum_{u=1}^{N_{\mathrm{P}}}\sum_{m=1}^{M}\sum_{n=1}^{N}\sum_{v=0}^{L-1}\left|\bar{y}^{u}_{k_i,mn}(t)\left(\bar{y}^{u}_{k_i,mn}(t+N_{\mathrm{C}})\right)^{*}\right|}{2\sum_{u=1}^{N_{\mathrm{P}}}\sum_{m=1}^{M}\sum_{n=1}^{N}\sum_{t=0}^{L-1}\left(\left|\bar{y}^{u}_{k_i,mn}(t)\right|-\left|\bar{y}^{u}_{k_i,mn}(t+N_{\mathrm{C}})\right|\right)^{2}}, \tag{36}$$

which is derived in Appendix E. Hence, we complete the calculation of $\rho^{ue}_{\mathrm{H},k_i}$. In the same fashion, $\rho^{ue}_{\mathrm{G},k_i}$ is estimated from the channel estimation error in the downlink channel.

5 Simulations and discussion

In the following simulations, system parameters are chosen as follows: digital modulation quadrature phase shift keying (QPSK), carrier frequency $f_{\mathrm{c}} = 900$ MHz, channel bandwidth BW = 1 MHz, $N_{\mathrm{C}} = 64$, the length of CP being 8, one RS and three pairs of users ($K = 3$) with each MS having three antennas ($M = 3$). The average SNRs at the RS and MSs are defined as $\mathrm{SNR}_{\mathrm{RS}} = P_{\mathrm{MS}}/\sigma^2_{\mathrm{RS}}$ and $\mathrm{SNR}_{\mathrm{MS}} = P_{\mathrm{RS}}/\sigma^2_{\mathrm{MS}}$, respectively. In the following, the normalized Doppler spread (NDS) is defined as $f_{\mathrm{d}}T$, where T denotes the length of the useful OFDM symbol. We define $\Delta m f_{\mathrm{d}} T_{\mathrm{s}}$, where T_{s} is the total length of the OFDM symbol including CP, and $\Delta m T_{\mathrm{s}}$ is the delayed time difference between channel estimation and beamforming at the RS.

Figs. 1–3 display the curves of the BER versus SNR of the proposed adaptive robust beamformer with $\Delta m f_{\mathrm{d}} T_{\mathrm{s}} = 0.01$ for three different values of α ($\alpha = 0.5, 1.0, 2.0$). From these figures, we find that four beamformers have increasing order in terms of BER performance: CSI mismatched, fixed ρ_{H} and ρ_{G}, proposed adaptive robust algorithm, and ideal CSI. Considering that the ideal CSI is in general not available in practice, the proposed method performs the best among the three practical methods and achieves 3 dB SNR gains over two others (fixed

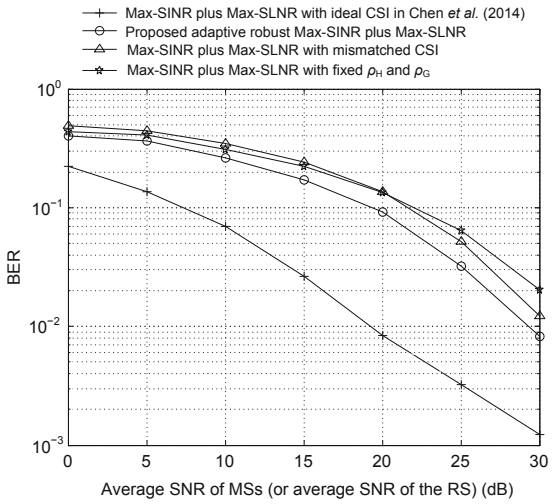

Fig. 1 Curves of BER versus SNR of the proposed adaptive robust beamformer and existing non-adaptive ones ($\boldsymbol{\alpha_{\mathrm{H}} = \alpha_{\mathrm{G}} = 0.5, \Delta m f_{\mathrm{d}} T_{\mathrm{s}} = 0.01}$)

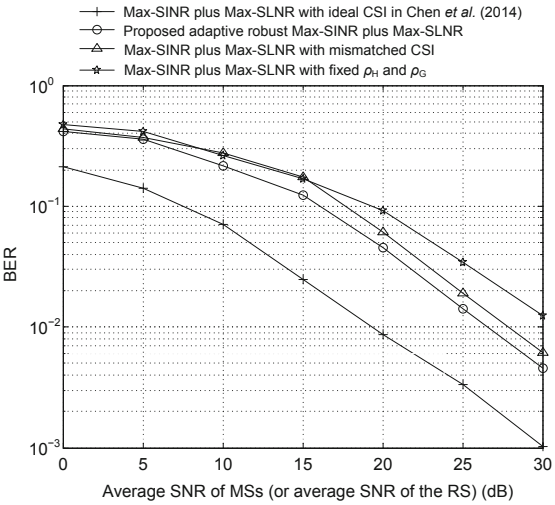

Fig. 2 Curves of BER versus SNR of the proposed adaptive robust beamformer and existing non-adaptive ones ($\boldsymbol{\alpha_{\mathrm{H}} = \alpha_{\mathrm{G}} = 1.0, \Delta m f_{\mathrm{d}} T_{\mathrm{s}} = 0.01}$)

ρ_{H} and ρ_{G} and mismatched cases) at BER=10^{-1}. Given a fixed $\Delta m f_{\mathrm{d}} T_{\mathrm{s}} = 0.01$, the BER performance of the proposed beamformer tends to the ideal BER performance as α increases from 0.5 to 2.0.

Figs. 4–6 show the curves of BER versus SNR of the proposed adaptive robust beamformer with $\Delta m f_{\mathrm{d}} T_{\mathrm{s}} = 0.05$ for three different values of α ($\alpha = 0.5, 1.0, 2.0$). From these figures, we find that the BER performances of all beamformers become worse due to the increase of time variation in the channel as $\Delta m f_{\mathrm{d}} T_{\mathrm{s}}$ increases from 0.01 to 0.05. The BER performance order among four beamformers in Fig. 5 is preserved in Fig. 6. This further verifies

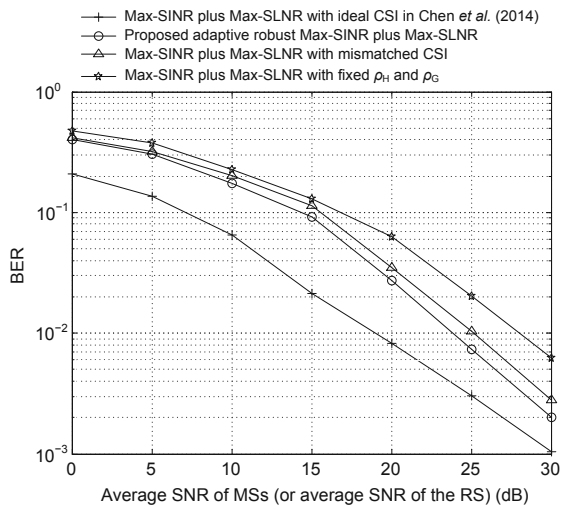

Fig. 3 Curvers of BER versus SNR of the proposed adaptive robust beamformer and existing non-adaptive ones ($\alpha_H = \alpha_G = 2.0, \Delta m f_d T_s = 0.01$)

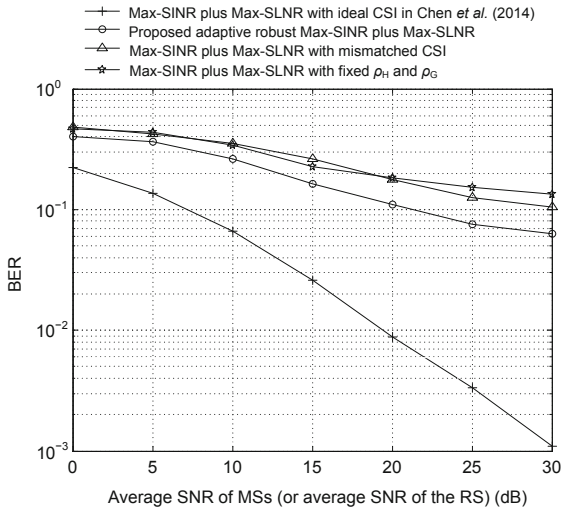

Fig. 4 Curves of BER versus SNR of the proposed adaptive robust beamformer and existing non-adaptive ones ($\alpha_H = \alpha_G = 0.5, \Delta m f_d T_s = 0.05$)

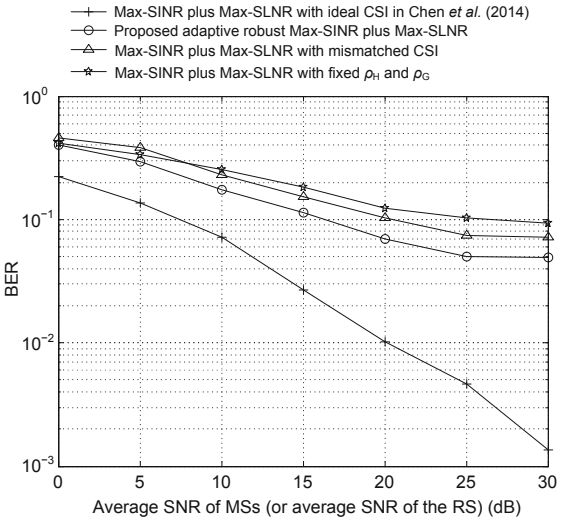

Fig. 5 Curves of BER versus SNR of the proposed adaptive robust beamformer and existing non-adaptive ones ($\alpha_H = \alpha_G = 1.0, \Delta m f_d T_s = 0.05$)

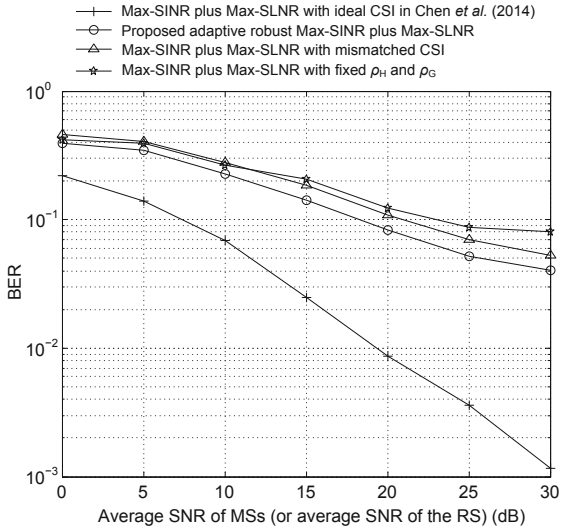

Fig. 6 Curves of BER versus SNR of the proposed adaptive robust beamformer and existing non-adaptive ones ($\alpha_H = \alpha_G = 2.0, \Delta m f_d T_s = 0.05$)

the fact that our method is more robust to some uncertainty or possible variation in the channel matrix from Doppler spread and channel estimation, compared to the other two non-ideal methods (fixed ρ_H and ρ_G and mismatched cases).

From Figs. 1–6, we find that for a given BER$= 10^{-1}$, the SNR gain achieved by the proposed method over other methods varies from 1 dB to 5 dB.

Fig. 7 plots the curves of average sum-rate versus α for the proposed adaptive robust beamformer with $\Delta m f_d T_s = 0.01$ for three different values of SNR (5, 15, and 25 dB). From Fig. 7, with increase in the value of α by increasing the number of pilot symbols, the sum-rate of our method converges to the ideal case as an upper bound, whereas the convergence rate grows with the value of SNR for given α and $\Delta m f_d T_s$. It is noted that the larger the α, the higher the channel estimation accuracy.

Finally, Fig. 8 illustrates the curves of BER versus α for the proposed method with $\Delta m f_d T_s = 0.01$ for three different values of SNR (5, 15, and 25 dB). From this figure, we can obtain the same trend as shown in Fig. 7.

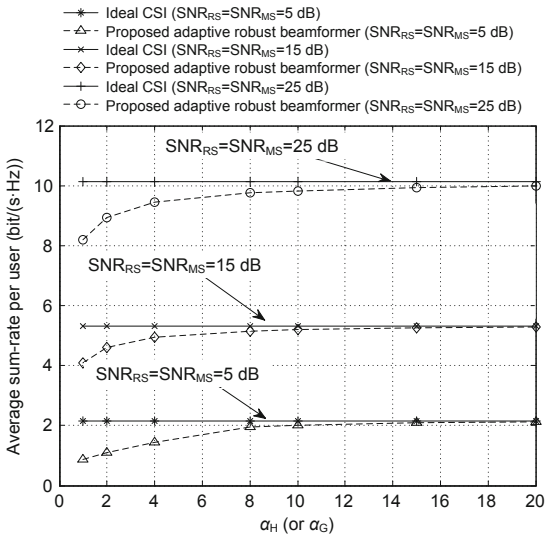

Fig. 7 Curves of sum-rate versus α in terms of the proposed adaptive robust beamformer at $\mathbf{SNR_{RS}}$=$\mathbf{SNR_{MS}}$=5 dB, 15 dB, 25 dB ($\Delta m f_d T_s = 0.01$)

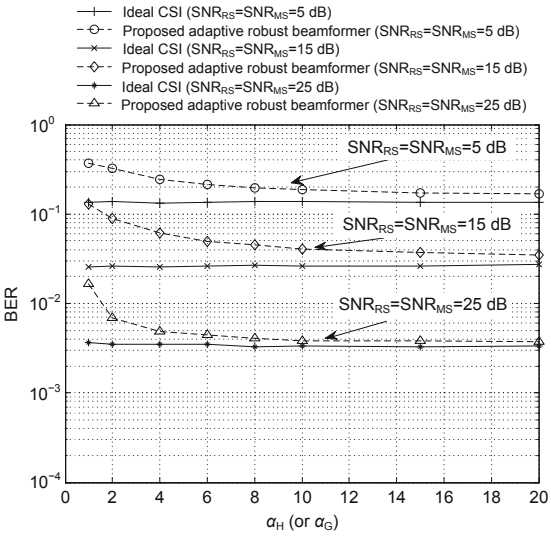

Fig. 8 Curves of BER versus α of the proposed adaptive robust beamformer at $\mathbf{SNR_{RS}}$=$\mathbf{SNR_{MS}}$=5 dB, 15 dB, 25 dB ($\Delta m f_d T_s = 0.01$)

6 Conclusions

In this paper, by real-time estimation of Doppler spread and SNR in the channel, an adaptive robust Max-SINR plus Max-SLNR beamformer at an RS is proposed to take into account some uncertainty or possible variation in the channel matrix induced from Doppler spread and channel estimation. From simulation results and analysis, we find that the proposed robust method can adaptively track channel variation and performs much better than existing robust and non-robust Max-SINR plus Max-SLNR nonadaptive schemes.

References

Aziz, A., Thron, C., Cui, S.G., *et al.*, 2014. Linearized robust beamforming for two-way relay systems. *IEEE Signal Process. Lett.*, **21**(8):1017-1021. http://dx.doi.org/10.1109/LSP.2014.2322118

Baddour, K.E., Beaulieu, N.C., 2003. Nonparametric Doppler spread estimation for flat fading channels. Proc. IEEE Wireless Communications and Networking Conf., p.953-958. http://dx.doi.org/10.1109/WCNC.2003.1200500

Chalise, B.K., Vandendorpe, L., 2009. MIMO relay design for multipoint-to-multipoint communications with imperfect channel state information. *IEEE Trans. Signal Process.*, **57**(7):2785-2796. http://dx.doi.org/10.1109/TSP.2009.2018610

Chen, Y., Shu, F., Wang, J., *et al.*, 2014. High-performance beamforming and spatial channel pairing schemes at relay station for AF-based multi-pair two-way relay networks. Proc. 6th Int. Conf. on Wireless Communications and Signal Processing, p.1-4. http://dx.doi.org/10.1109/WCSP.2014.6992011

Cover, T., Gamal, A.E., 1979. Capacity theorems for the relay channel. *IEEE Trans. Inform. Theory*, **25**(5):572-584. http://dx.doi.org/10.1109/TIT.1979.1056084

Degenhardt, H., Klein, A., 2012. Self-interference aware MIMO filter design for non-regenerative multi-pair two-way relaying. Proc. IEEE Wireless Communications and Networking Conf., p.272-276. http://dx.doi.org/10.1109/WCNC.2012.6214264

Holtzman, J.M., Sampath, A., 1995. Adaptive averaging methodology for handoffs in cellular systems. *IEEE Trans. Veh. Technol.*, **44**(1):59-66. http://dx.doi.org/10.1109/25.350270

Ijaz, A., Awoseyila, A.B., Evans, B.G., 2011. Low-complexity time-domain SNR estimation for OFDM systems. *Electron. Lett.*, **47**(20):1154-1156. http://dx.doi.org/10.1049/el.2011.2014

Knopp, R., 2007. Two-way wireless communication via a relay station. GDR-ISIS Meeting.

Kramer, G., Gastpar, M., Gupta, P., 2005. Cooperative strategies and capacity theorems for relay networks. *IEEE Trans. Inform. Theory*, **51**(9):3037-3063. http://dx.doi.org/10.1109/TIT.2005.853304

Laneman, J.N., Wornell, G.W., 2003. Distributed space-time-coded protocols for exploiting cooperative diversity in wireless networks. *IEEE Trans. Inform. Theory*, **49**(10):2415-2425. http://dx.doi.org/10.1109/TIT.2003.817829

Mao, J.L., Gao, J.C., Liu, Y.A., *et al.*, 2012. Robust multiuser MIMO scheduling algorithms with imperfect CSI. *Sci. China Inform. Sci.*, **55**(4):815-826. http://dx.doi.org/10.1007/s11432-011-4388-3

Popovski, P., Yomo, H., 2006. Bi-directional amplification of throughput in a wireless multi-hop network. Proc. IEEE 63rd Vehicular Technology Conf., p.588-593. http://dx.doi.org/10.1109/VETECS.2006.1682892

Rankov, B., Wittneben, A., 2007. Spectral efficient protocols for half-duplex fading relay channels. *IEEE J. Sel. Areas Commun.*, **25**(2):379-389. http://dx.doi.org/10.1109/JSAC.2007.070213

Sadek, M., Tarighat, A., Sayed, A.H., 2007. A leakage-based precoding scheme for downlink multi-user MIMO channels. *IEEE Trans. Wirel. Commun.*, **6**(5):1711-1721. http://dx.doi.org/10.1109/TWC.2007.360373

Sendonaris, A., Erkip, E., Aazhang, B., 2003. User cooperation diversity. Part I: system description. *IEEE Trans. Commun.*, **51**(11):1927-1938. http://dx.doi.org/10.1109/TCOMM.2003.818096

Shen, H., Wang, J.H., Levy, B.C., *et al.*, 2013. Robust optimization for amplify-and-forward MIMO relaying from a worst-case perspective. *IEEE Trans. Signal Process.*, **61**(21):5458-5471. http://dx.doi.org/10.1109/TSP.2013.2278819

Shu, F., Chen, Y., You, X.H., *et al.*, 2014a. Low-complexity optimal spatial channel pairing for AF-based multi-pair two-way relay networks. *Sci. China Inform. Sci.*, **57**(10):1-10. http://dx.doi.org/10.1007/s11432-014-5102-z

Shu, F., Lu, Y.Z., Chen, Y., *et al.*, 2014b. High-sum-rate beamformers for multi-pair two-way relay networks with amplify-and-forward relaying strategy. *Sci. China Inform. Sci.*, **57**(2):1-11. http://dx.doi.org/10.1007/s11432-013-4980-9

Tepedelenlioglu, C., Giannakis, G.B., 2001. On velocity estimation and correlation properties of narrow-band mobile communication channels. *IEEE Trans. Veh. Technol.*, **50**(4):1039-1052. http://dx.doi.org/10.1109/25.938579

Wang, C., Au, E.K.S., Murch, R.D., *et al.*, 2007. On the performance of the MIMO zero-forcing receiver in the presence of channel estimation error. *IEEE Trans. Wirel. Commun.*, **6**(3):805-810. http://dx.doi.org/10.1109/TWC.2007.05384

Wang, C.Y., Liu, T.C.K., Dong, X.D., 2012. Impact of channel estimation error on the performance of amplify-and-forward two-way relaying. *IEEE Trans. Veh. Technol.*, **61**(3):1197-1207. http://dx.doi.org/10.1109/TVT.2012.2185964

Wang, J., Wen, O.Y., Li, S.Q., 2008. Soft-output MMSE MIMO detector under imperfect channel estimation. Proc. IEEE Wireless Communications and Networking Conf., p.1334-1338. http://dx.doi.org/10.1109/WCNC.2008.240

Yilmaz, E., Zakhour, R., Gesbert, D., *et al.*, 2010. Multi-pair two-way relay channel with multiple antenna relay station. Proc. IEEE Int. Conf. on Communications, p.1-5. http://dx.doi.org/10.1109/ICC.2010.5502396

Zhang, R., Liang, Y.C., Chai, C.C., *et al.*, 2009. Optimal beamforming for two-way multi-antenna relay channel with analogue network coding. *IEEE J. Sel. Areas Commun.*, **27**(5):699-712. http://dx.doi.org/10.1109/JSAC.2009.090611

Zheng, F., Hua, Y., Koshy, J.C., 2006. Joint source and relay optimization for a non-regenerative MIMO relay. Proc. 4th IEEE Workshop on Sensor Array and Multichannel Processing, p.239-243. http://dx.doi.org/10.1109/SAM.2006.1706129

Zhong, B., Zhang, X., Li, Y., *et al.*, 2013. Impact of partial relay selection on the capacity of communications systems with outdated CSI and adaptive transmission techniques. Proc. IEEE Wireless Communications and Networking Conf., p.3720-3725. http://dx.doi.org/10.1109/WCNC.2013.6555166

Zhou, B.L., Jiang, L.G., Zhang, L., *et al.*, 2011. Impact of imperfect channel state information on TDD downlink multiuser MIMO system. Proc. IEEE Wireless Communications and Networking Conf., p.1823-1828. http://dx.doi.org/10.1109/WCNC.2011.5779410

Appendix A: Derivation of the proposed robust Max-SINR

To derive the simple form of matrix $\boldsymbol{A}_{k_{(-i)}}$ in Eq. (16), it is obvious that three conditional expected values $\boldsymbol{\Phi}_1$, $\boldsymbol{\Phi}_2$, and $\boldsymbol{\Phi}_3$ should be first computed. Conditioned on $\widehat{\boldsymbol{H}}^{(u-\Delta u)q}$ and ρ^u_{H,k_i}, we have the expression in Eq. (A1) (see p.276).

In Eq. (A1), similar to Wang *et al.* (2008), $E\left[\boldsymbol{H}^{uq}_{\mathrm{e},k_{(-i)}}\left(\boldsymbol{H}^{uq}_{\mathrm{e},k_{(-i)}}\right)^{\mathrm{H}}\middle|\rho^u_{\mathrm{H},k_{(-i)}},\widehat{\boldsymbol{H}}^{(u-\Delta u)q}_{k_{(-i)}}\right]$ can be represented as

$$E\left[\boldsymbol{H}^{uq}_{\mathrm{e},k_{(-i)}}\left(\boldsymbol{H}^{uq}_{\mathrm{e},k_{(-i)}}\right)^{\mathrm{H}}\middle|\rho^u_{\mathrm{H},k_{(-i)}},\widehat{\boldsymbol{H}}^{(u-\Delta u)q}_{k_{(-i)}}\right]$$
$$=\sum_{n=1}^{N}E\left(\boldsymbol{h}^{uq}_{\mathrm{e},k_{(-i)}n}\left(\boldsymbol{h}^{uq}_{\mathrm{e},k_{(-i)}n}\right)^{\mathrm{H}}\middle|\rho^u_{\mathrm{H},k_{(-i)}},\widehat{\boldsymbol{H}}^{(u-\Delta u)q}_{k_{(-i)}}\right),\tag{A2}$$

where $\boldsymbol{h}_{\mathrm{e},k_{(-i)}n}$ and $\boldsymbol{h}^{\mathrm{H}}_{\mathrm{e},k_{(-i)}n}$ denote the nth column of matrices $\boldsymbol{H}_{\mathrm{e},k_{(-i)}}$ and $\boldsymbol{H}^{\mathrm{H}}_{\mathrm{e},k_{(-i)}}$, respectively. The conditional correlation matrix

$$E\left(\boldsymbol{h}^{uq}_{\mathrm{e},k_{(-i)}n}\left(\boldsymbol{h}^{uq}_{\mathrm{e},k_{(-i)}n}\right)^{\mathrm{H}}\middle|\rho^u_{\mathrm{H},k_{(-i)}},\widehat{\boldsymbol{H}}^{(u-\Delta u)q}_{k_{(-i)}}\right)$$

in Eq. (A2) can be expressed as

$$E\left(\boldsymbol{h}^{uq}_{\mathrm{e},k_{(-i)}n}\left(\boldsymbol{h}^{uq}_{\mathrm{e},k_{(-i)}n}\right)^{\mathrm{H}}\middle|\rho^u_{\mathrm{H},k_{(-i)}},\widehat{\boldsymbol{H}}^{(u-\Delta u)q}_{k_{(-i)}}\right)$$
$$=\mathrm{cov}\left[\boldsymbol{h}^{uq}_{\mathrm{e},k_{(-i)}n}\left(\boldsymbol{h}^{uq}_{\mathrm{e},k_{(-i)}n}\right)^{\mathrm{H}}\middle|\rho^u_{\mathrm{H},k_{(-i)}},\widehat{\boldsymbol{H}}^{(u-\Delta u)q}_{k_{(-i)}}\right]$$
$$+E\left[\boldsymbol{h}^{uq}_{\mathrm{e},k_{(-i)}n}\middle|\rho^u_{\mathrm{H},k_{(-i)}},\widehat{\boldsymbol{H}}^{(u-\Delta u)q}_{k_{(-i)}}\right]$$
$$\cdot E\left[\left(\boldsymbol{h}^{uq}_{\mathrm{e},k_{(-i)}n}\right)^{\mathrm{H}}\middle|\rho^u_{\mathrm{H},k_{(-i)}},\widehat{\boldsymbol{H}}^{(u-\Delta u)q}_{k_{(-i)}}\right],\tag{A3}$$

$$\begin{aligned}\boldsymbol{\Phi}_1 &= E\left[\boldsymbol{H}^{uq}_{k_{(-i)}}\left(\boldsymbol{H}^{uq}_{k_{(-i)}}\right)^{\mathrm{H}}\middle|\rho^{u}_{\mathrm{H},k_{(-i)}},\widehat{\boldsymbol{H}}^{(u-\Delta u)q}_{k_{(-i)}}\right]\\ &= \frac{1}{\left(\rho^{u}_{\mathrm{H},k_{(-i)}}\right)^2}\widehat{\boldsymbol{H}}^{(u-\Delta u)q}_{k_{(-i)}}\left(\widehat{\boldsymbol{H}}^{(u-\Delta u)q}_{k_{(-i)}}\right)^{\mathrm{H}} - \frac{\xi^{u}_{\mathrm{H},k_{(-i)}}}{\left(\rho^{u}_{\mathrm{H},k_{(-i)}}\right)^2}\cdot\widehat{\boldsymbol{H}}^{(u-\Delta u)q}_{k_{(-i)}}E\left[\left(\boldsymbol{H}^{uq}_{\mathrm{e},k_{(-i)}}\right)^{\mathrm{H}}\middle|\rho^{u}_{\mathrm{H},k_{(-i)}},\widehat{\boldsymbol{H}}^{(u-\Delta u)q}_{k_{(-i)}}\right]\\ &\quad - \frac{\xi^{u}_{\mathrm{H},k_{(-i)}}}{\left(\rho^{u}_{\mathrm{H},k_{(-i)}}\right)^2}E\left[\boldsymbol{H}^{uq}_{\mathrm{e},k_{(-i)}}\middle|\rho^{u}_{\mathrm{H},k_{(-i)}},\widehat{\boldsymbol{H}}^{(u-\Delta u)q}_{k_{(-i)}}\right]\cdot\left(\widehat{\boldsymbol{H}}^{(u-\Delta u)q}_{k_{(-i)}}\right)^{\mathrm{H}} + \frac{\left(\xi^{u}_{\mathrm{H},k_{(-i)}}\right)^2}{\left(\rho^{u}_{\mathrm{H},k_{(-i)}}\right)^2}\\ &\quad\cdot E\left[\boldsymbol{H}^{uq}_{\mathrm{e},k_{(-i)}}\left(\boldsymbol{H}^{uq}_{\mathrm{e},k_{(-i)}}\right)^{\mathrm{H}}\middle|\rho^{u}_{\mathrm{H},k_{(-i)}},\widehat{\boldsymbol{H}}^{(u-\Delta u)q}_{k_{(-i)}}\right].\end{aligned}\tag{A1}$$

$$\operatorname{cov}\left[\boldsymbol{h}^{uq}_{\mathrm{e},k_{(-i)}n}\left(\boldsymbol{h}^{uq}_{\mathrm{e},k_{(-i)}n}\right)^{\mathrm{H}}\middle|\rho^{u}_{\mathrm{H},k_{(-i)}},\widehat{\boldsymbol{H}}^{(u-\Delta u)q}_{k_{(-i)}}\right] = \frac{\sigma^2_{\mathrm{H}}\left(\rho^{u}_{\mathrm{H},k_{(-i)}}\right)^2}{\left(\xi^{u}_{\mathrm{H},k_{(-i)}}\right)^2\sigma^2_{\mathrm{H}} + \left(\rho^{u}_{\mathrm{H},k_{(-i)}}\right)^2}\boldsymbol{I}_N.\tag{A6}$$

$$\begin{aligned}&E\left[\boldsymbol{H}^{uq}_{\mathrm{e},k_{(-i)}}\left(\boldsymbol{H}^{uq}_{\mathrm{e},k_{(-i)}}\right)^{\mathrm{H}}\middle|\rho^{u}_{\mathrm{H},k_{(-i)}},\widehat{\boldsymbol{H}}^{(u-\Delta u)q}_{k_{(-i)}}\right]\\ =&\frac{N\sigma^2_{\mathrm{H}}\left(\rho^{u}_{\mathrm{H},k_{(-i)}}\right)^2}{\left(\xi^{u}_{\mathrm{H},k_{(-i)}}\right)^2\sigma^2_{\mathrm{H}} + \left(\rho^{u}_{\mathrm{H},k_{(-i)}}\right)^2}\boldsymbol{I}_N + \left(\frac{\sigma^2_{\mathrm{H}}}{\left(\xi^{u}_{\mathrm{H},k_{(-i)}}\right)^2\sigma^2_{\mathrm{H}} + \left(\rho^{u}_{\mathrm{H},k_{(-i)}}\right)^2}\right)^2\widehat{\boldsymbol{H}}^{(u-\Delta u)q}_{k_{(-i)}}\left(\widehat{\boldsymbol{H}}^{(u-\Delta u)q}_{k_{(-i)}}\right)^{\mathrm{H}}.\end{aligned}\tag{A7}$$

where $\operatorname{cov}(\cdot)$ denotes the operator of the covariance matrix. Considering that each element of $\boldsymbol{H}$ has independent real and imaginary parts with zero mean and one half (unit) variance, we have

$$\begin{aligned}&E\left[\boldsymbol{h}^{uq}_{\mathrm{e},k_{(-i)}n}\middle|\rho^{u}_{\mathrm{H},k_{(-i)}},\widehat{\boldsymbol{H}}^{(u-\Delta u)q}_{k_{(-i)}}\right]\\ =&E\left[\boldsymbol{h}^{uq}_{\mathrm{e},k_{(-i)}n}\left(\boldsymbol{h}^{uq}_{\mathrm{e},k_{(-i)}n}\right)^{\mathrm{H}}\right]\\ =&\frac{\sigma^2_{\mathrm{H}}}{\left(\xi^{u}_{\mathrm{H},k_{(-i)}}\right)^2\sigma^2_{\mathrm{H}} + \left(\rho^{u}_{\mathrm{H},k_{(-i)}}\right)^2}\widehat{\boldsymbol{h}}^{(u-\Delta u)q}_{k_{(-i)}n}\end{aligned}\tag{A4}$$

and

$$\begin{aligned}&E\left[\left(\boldsymbol{h}^{uq}_{\mathrm{e},k_{(-i)}n}\right)^{\mathrm{H}}\middle|\rho^{u}_{\mathrm{H},k_{(-i)}},\widehat{\boldsymbol{H}}^{(u-\Delta u)q}_{k_{(-i)}}\right]\\ =&\frac{\sigma^2_{\mathrm{H}}}{\left(\xi^{u}_{\mathrm{H},k_{(-i)}}\right)^2\sigma^2_{\mathrm{H}} + \left(\rho^{u}_{\mathrm{H},k_{(-i)}}\right)^2}\left(\widehat{\boldsymbol{h}}^{(u-\Delta u)q}_{k_{(-i)}n}\right)^{\mathrm{H}}.\end{aligned}\tag{A5}$$

In Eq. (A3), the correlation matrix

$$\operatorname{cov}\left[\boldsymbol{h}^{uq}_{\mathrm{e},k_{(-i)}n}\left(\boldsymbol{h}^{uq}_{\mathrm{e},k_{(-i)}n}\right)^{\mathrm{H}}\middle|\rho^{u}_{\mathrm{H},k_{(-i)}},\widehat{\boldsymbol{H}}^{(u-\Delta u)q}_{k_{(-i)}}\right]$$

can be simplified to Eq. (A6) (Wang *et al.*, 2008). Substituting Eqs. (A3)–(A6) into Eq. (A2) yields Eq. (A7).

Similarly, we can obtain

$$\begin{aligned}&E\left[\boldsymbol{H}^{uq}_{\mathrm{e},k_{(-i)}}\middle|\rho^{u}_{\mathrm{H},k_{(-i)}},\widehat{\boldsymbol{H}}^{(u-\Delta u)q}_{k_{(-i)}}\right]\\ =&\frac{\sigma^2_{\mathrm{H}}}{\left(\xi^{u}_{\mathrm{H},k_{(-i)}}\right)^2\sigma^2_{\mathrm{H}} + \left(\rho^{u}_{\mathrm{H},k_{(-i)}}\right)^2}\widehat{\boldsymbol{H}}^{(u-\Delta u)q}_{k_{(-i)}},\end{aligned}\tag{A8}$$

$$\begin{aligned}&E\left[\left(\boldsymbol{H}^{uq}_{\mathrm{e},k_{(-i)}}\right)^{\mathrm{H}}\middle|\rho^{u}_{\mathrm{H},k_{(-i)}},\widehat{\boldsymbol{H}}^{(u-\Delta u)q}_{k_{(-i)}}\right]\\ =&\frac{\sigma^2_{\mathrm{H}}}{\left(\xi^{u}_{\mathrm{H},k_{(-i)}}\right)^2\sigma^2_{\mathrm{H}} + \left(\rho^{u}_{\mathrm{H},k_{(-i)}}\right)^2}\left(\widehat{\boldsymbol{H}}^{(u-\Delta u)q}_{k_{(-i)}}\right)^{\mathrm{H}}.\end{aligned}\tag{A9}$$

Substituting Eqs. (A7)–(A9) into Eq. (A1) yields Eq. (A10).

In the same way, we have $\boldsymbol{\Phi}_2$ (Eq. (A11)) and $\boldsymbol{\Phi}_3$ (Eq. (A12)). Thus, substituting Eqs. (A10)–(A12) into matrix $\boldsymbol{A}_{k_{(-i)}}$ (Eq. (16)) yields Eq. (A13) (see p.278). This completes the derivation of matrix $\boldsymbol{A}_{k_{(-i)}}$.

Appendix B: Derivation of the proposed robust Max-SLNR

Observing $\boldsymbol{A}_{k_{(-i)}}$ (Eq. (16)) and $\boldsymbol{B}_{k_i}$ (Eq. (22)), we find that they have the same structure and form. This also implies the duality between Max-SINR over uplink and Max-SLNR over downlink. As derived in Appendix A, we have to first calculate the three expected values corresponding to matrix $\boldsymbol{B}_{k_i}$ in Eq. (22). Similar to Eq. (A10) in Appendix A, we have

$$\begin{aligned}\boldsymbol{\Psi}_1 =&E\left[\left(\boldsymbol{G}_{k_i}^{uq}\right)^*\left(\boldsymbol{G}_{k_i}^{uq}\right)^{\mathrm{T}}\middle|\rho_{\mathrm{G},k_i}^u,\widehat{\boldsymbol{G}}_{k_i}^{(u-\Delta u)q}\right]\\ =&\left(\frac{\sigma_{\mathrm{G}}^2\xi_{\mathrm{G},k_i}^u}{\left(\xi_{\mathrm{G},k_i}^u\right)^2\rho_{\mathrm{G},k_i}^u\sigma_{\mathrm{G}}^2+\left(\rho_{\mathrm{G},k_i}^u\right)^3}\right.\\ &\left.-\frac{1}{\rho_{\mathrm{G},k_i}^u}\right)^2\left(\widehat{\boldsymbol{G}}_{k_i}^{(u-\Delta u)q}\right)^*\left(\widehat{\boldsymbol{G}}_{k_i}^{(u-\Delta u)q}\right)^{\mathrm{T}}\\ &+\frac{N\sigma_{\mathrm{G}}^2\left(\xi_{\mathrm{G},k_i}^u\right)^2}{\left(\xi_{\mathrm{G},k_i}^u\right)^2\sigma_{\mathrm{G}}^2+\left(\rho_{\mathrm{G},k_i}^u\right)^2}\boldsymbol{I}_N.\end{aligned}\tag{B1}$$

$$\begin{aligned}\boldsymbol{\Phi}_1 =&E\left[\boldsymbol{H}_{k_{(-i)}}^{uq}\left(\boldsymbol{H}_{k_{(-i)}}^{uq}\right)^{\mathrm{H}}\middle|\rho_{\mathrm{H},k_{(-i)}}^u,\widehat{\boldsymbol{H}}_{k_{(-i)}}^{(u-\Delta u)q}\right]=\left(\frac{\sigma_{\mathrm{H}}^2\xi_{\mathrm{H},k_{(-i)}}^u}{\left(\xi_{\mathrm{H},k_{(-i)}}^u\right)^2\rho_{\mathrm{H},k_{(-i)}}^u\sigma_{\mathrm{H}}^2+\left(\rho_{\mathrm{H},k_{(-i)}}^u\right)^3}-\frac{1}{\rho_{\mathrm{H},k_{(-i)}}^u}\right)^2\\ &\cdot\widehat{\boldsymbol{H}}_{k_{(-i)}}^{(u-\Delta u)q}\left(\widehat{\boldsymbol{H}}_{k_{(-i)}}^{(u-\Delta u)q}\right)^{\mathrm{H}}+\frac{N\sigma_{\mathrm{H}}^2\left(\xi_{\mathrm{H},k_{(-i)}}^u\right)^2}{\left(\xi_{\mathrm{H},k_{(-i)}}^u\right)^2\sigma_{\mathrm{H}}^2+\left(\rho_{\mathrm{H},k_{(-i)}}^u\right)^2}\boldsymbol{I}_N.\end{aligned}\tag{A10}$$

$$\begin{aligned}\boldsymbol{\Phi}_2 =&E\left[\left(\boldsymbol{G}_{-k}^{uq}\right)^*\left(\boldsymbol{G}_{-k}^{uq}\right)^{\mathrm{T}}\middle|\left\{\rho_{\mathrm{G},1_a}^u,\rho_{\mathrm{G},1_b}^u,\ldots,\rho_{\mathrm{G},(k-1)_b}^u,\rho_{\mathrm{G},(k+1)_a}^u,\ldots,\rho_{\mathrm{G},K_a}^u,\rho_{\mathrm{G},K_b}^u\right\},\widehat{\boldsymbol{G}}_{-k}^{(u-\Delta u)q}\right]\\ =&\sum_{k'=1,k'\neq k}^{K}\sum_{i'\in\{a,b\}}\left(\frac{\sigma_{\mathrm{H}}^2\xi_{\mathrm{H},k_{i'}'}^u}{\left(\xi_{\mathrm{H},k_{i'}'}^u\right)^2\rho_{\mathrm{H},k_{i'}'}^u\sigma_{\mathrm{H}}^2+\left(\rho_{\mathrm{H},k_{i'}'}^u\right)^3}-\frac{1}{\rho_{\mathrm{H},k_{i'}'}^u}\right)^2\widehat{\boldsymbol{H}}_{k_{i'}'}^{(u-\Delta u)q}\left(\widehat{\boldsymbol{H}}_{k_{i'}'}^{(u-\Delta u)q}\right)^{\mathrm{H}}\\ &+\sum_{k'=1,k'\neq k}^{K}\sum_{i'\in\{a,b\}}\frac{N\sigma_{\mathrm{H}}^2\left(1-\left(\rho_{\mathrm{H},k_{i'}'}^u\right)^2\right)}{\left(\xi_{\mathrm{H},k_{i'}'}^u\right)^2\sigma_{\mathrm{H}}^2+\left(\rho_{\mathrm{H},k_{i'}'}^u\right)^2}\boldsymbol{I}_N.\end{aligned}\tag{A11}$$

$$\begin{aligned}\boldsymbol{\Phi}_3 =&E\left[\boldsymbol{H}_{\mathrm{e},k_i}^{uq}\left(\boldsymbol{H}_{\mathrm{e},k_i}^{uq}\right)^{\mathrm{H}}\middle|\rho_{\mathrm{H},k_i}^u,\widehat{\boldsymbol{H}}_{k_i}^{(u-\Delta u)q}\right]\\ =&\left(\frac{\sigma_{\mathrm{H}}^2\xi_{\mathrm{H},k_i}^u}{\left(\xi_{\mathrm{H},k_i}^u\right)^2\rho_{\mathrm{H},k_i}^u\sigma_{\mathrm{H}}^2+\left(\rho_{\mathrm{H},k_i}^u\right)^3}-\frac{1-\rho_{\mathrm{H},k_i}^u}{\rho_{\mathrm{H},k_i}^u}\right)^2\widehat{\boldsymbol{H}}_{k_i}^{(u-\Delta u)q}\left(\widehat{\boldsymbol{H}}_{k_i}^{(u-\Delta u)q}\right)^{\mathrm{H}}+\frac{N\sigma_{\mathrm{H}}^2\left(\xi_{\mathrm{H},k_i}^u\right)^2}{\left(\xi_{\mathrm{H},k_i}^u\right)^2\sigma_{\mathrm{H}}^2+\left(\rho_{\mathrm{H},k_i}^u\right)^2}\boldsymbol{I}_N.\end{aligned}\tag{A12}$$

$$\boldsymbol{A}_{k_{(-i)}}=\Bigg\{\left(\frac{\sigma_{\mathrm{H}}^2\xi_{\mathrm{H},k_{(-i)}}^u}{\left(\xi_{\mathrm{H},k_{(-i)}}^u\right)^2\rho_{\mathrm{H},k_{(-i)}}^u\sigma_{\mathrm{H}}^2+\left(\rho_{\mathrm{H},k_{(-i)}}^u\right)^3}-\frac{1}{\rho_{\mathrm{H},k_{(-i)}}^u}\right)^2\left(\widehat{\boldsymbol{H}}_{k_{(-i)}}^{(u-\Delta u)q}\right)^*\left(\widehat{\boldsymbol{H}}_{k_{(-i)}}^{(u-\Delta u)q}\right)^{\mathrm{T}}$$
$$+\frac{N\sigma_{\mathrm{H}}^2\left(\xi_{\mathrm{H},k_{(-i)}}^u\right)^2}{\left(\xi_{\mathrm{H},k_{(-i)}}^u\right)^2\sigma_{\mathrm{H}}^2+\left(\rho_{\mathrm{H},k_{(-i)}}^u\right)^2}\boldsymbol{I}_N\Bigg\}\Bigg\{\sigma_{\mathrm{MS}}^2\boldsymbol{I}_N+\frac{P_{\mathrm{MS}}}{M}\Bigg[\left(\frac{\sigma_{\mathrm{H}}^2\xi_{\mathrm{H},k_i}^u}{\left(\xi_{\mathrm{H},k_i}^u\right)^2\rho_{\mathrm{H},k_i}^u\sigma_{\mathrm{H}}^2+\left(\rho_{\mathrm{H},k_i}^u\right)^3}\right.$$
$$\left.-\frac{1-\rho_{\mathrm{H},k_i}^u}{\rho_{\mathrm{H},k_i}^u}\right)^2\left(\widehat{\boldsymbol{H}}_{k_i}^{(u-\Delta u)q}\right)^*\left(\widehat{\boldsymbol{H}}_{k_i}^{(u-\Delta u)q}\right)^{\mathrm{T}}+\frac{N\sigma_{\mathrm{H}}^2\left(\xi_{\mathrm{H},k_i}^u\right)^2}{\left(\xi_{\mathrm{H},k_i}^u\right)^2\sigma_{\mathrm{H}}^2+\left(\rho_{\mathrm{H},k_i}^u\right)^2}\boldsymbol{I}_N$$
$$+\sum_{k'=1,k'\neq k}^{K}\sum_{i'\in\{a,b\}}\left(\frac{\sigma_{\mathrm{H}}^2\xi_{\mathrm{H},k'_{i'}}^u}{\left(\xi_{\mathrm{H},k'_{i'}}^u\right)^2\rho_{\mathrm{H},k'_{i'}}^u\sigma_{\mathrm{H}}^2+\left(\rho_{\mathrm{H},k'_{i'}}^u\right)^3}-\frac{1}{\rho_{\mathrm{H},k'_{i'}}^u}\right)^2\left(\widehat{\boldsymbol{H}}_{k'_{i'}}^{(u-\Delta u)q}\right)^*\left(\widehat{\boldsymbol{H}}_{k'_{i'}}^{(u-\Delta u)q}\right)^{\mathrm{T}}$$
$$\left.+\sum_{k'=1,k'\neq k}^{K}\sum_{i'\in\{a,b\}}\frac{N\sigma_{\mathrm{H}}^2\left(\xi_{\mathrm{H},k'_{i'}}^u\right)^2}{\left(\xi_{\mathrm{H},k'_{i'}}^u\right)^2\sigma_{\mathrm{H}}^2+\left(\rho_{\mathrm{H},k'_{i'}}^u\right)^2}\boldsymbol{I}_N\right]\Bigg\}^{-1}. \tag{A13}$$

Similar to Eq. (A11) in Appendix A, we have

$$\boldsymbol{\Psi}_2=E\Bigg[(\boldsymbol{G}_{-k}^{uq})^*\left(\boldsymbol{G}_{-k}^{uq}\right)^{\mathrm{T}}\Bigg|\Big\{\rho_{\mathrm{G},1_a}^u,\rho_{\mathrm{G},1_b}^u,\ldots,$$
$$\rho_{\mathrm{G},(k-1)_b}^u,\rho_{\mathrm{G},(k+1)_a}^u,\ldots,\rho_{\mathrm{G},K_a}^u,\rho_{\mathrm{G},K_b}^u\Big\},\widehat{\boldsymbol{G}}_{-k}^{(u-\Delta u)q}\Bigg]$$
$$=\sum_{k'=1,k'\neq k}^{K}\sum_{i'\in\{a,b\}}\Bigg(\frac{\sigma_{\mathrm{G}}^2\xi_{\mathrm{G},k'_{i'}}^u}{\left(\xi_{\mathrm{G},k'_{i'}}^u\right)^2\rho_{\mathrm{G},k'_{i'}}^u\sigma_{\mathrm{G}}^2+\left(\rho_{\mathrm{G},k'_{i'}}^u\right)^3}$$
$$-\frac{1}{\rho_{\mathrm{G},k'_{i'}}^u}\Bigg)^2\left(\widehat{\boldsymbol{G}}_{k'_{i'}}^{(u-\Delta u)q}\right)^*\left(\widehat{\boldsymbol{G}}_{k'_{i'}}^{(u-\Delta u)q}\right)^{\mathrm{T}}$$
$$+\sum_{k'=1,k'\neq k}^{K}\sum_{i'\in\{a,b\}}\frac{N\sigma_{\mathrm{G}}^2\left(\xi_{\mathrm{G},k'_{i'}}^u\right)^2}{\left(\xi_{\mathrm{G},k'_{i'}}^u\right)^2\sigma_{\mathrm{G}}^2+\left(\rho_{\mathrm{G},k'_{i'}}^u\right)^2}\boldsymbol{I}_N. \tag{B2}$$

Similar to Eq. (A12) in Appendix A, we have

$$\boldsymbol{\Psi}_3=E\left[\left(\boldsymbol{H}_{\mathrm{e},k_i}^{uq}\right)^*\left(\boldsymbol{H}_{\mathrm{e},k_i}^{uq}\right)^{\mathrm{T}}\middle|\rho_{\mathrm{G},k_{(-i)}}^u,\widehat{\boldsymbol{G}}_{k_{(-i)}}^{(u-\Delta u)q}\right]$$
$$=\Bigg(\frac{\sigma_{\mathrm{G}}^2\xi_{\mathrm{G},k_{(-i)}}^u}{\left(\xi_{\mathrm{G},k_{(-i)}}^u\right)^2\rho_{\mathrm{G},k_{(-i)}}^u\sigma_{\mathrm{G}}^2+\left(\rho_{\mathrm{G},k_{(-i)}}^u\right)^3}$$
$$-\frac{1-\rho_{\mathrm{G},k_{(-i)}}^u}{\rho_{\mathrm{G},k_{(-i)}}^u}\Bigg)^2\left(\widehat{\boldsymbol{G}}_{k_{(-i)}}^{(u-\Delta u)q}\right)^*\left(\widehat{\boldsymbol{G}}_{k_{(-i)}}^{(u-\Delta u)q}\right)^{\mathrm{T}}$$
$$+\frac{N\sigma_{\mathrm{G}}^2\left(\xi_{\mathrm{G},k_{(-i)}}^u\right)^2}{\left(\xi_{\mathrm{G},k_{(-i)}}^u\right)^2\sigma_{\mathrm{G}}^2+\left(\rho_{\mathrm{G},k_{(-i)}}^u\right)^2}\boldsymbol{I}_N. \tag{B3}$$

Substituting Eqs. (B1)–(B3) into Eq. (22) yields Eq. (B4). This completes the derivation of matrix $\boldsymbol{B}_{k_i}$.

Appendix C: Derivation of $\boldsymbol{\rho}_{\mathrm{H},\boldsymbol{k_i}}^{\boldsymbol{ud}}$

In terms of the the MSE criterion, substituting Eq. (26) into Eq. (27) yields

$$E\left(\left|\tilde{Y}_{k_i,mn}^{uq}-\widehat{H}_{k_i,mn}^{uq}\tilde{s}_{k_i,m}^{uq}\right|^2\right)$$
$$=\Re_{\mathrm{HH},k_i}(0,0)-2\rho_{\mathrm{H},k_i}^{\mathrm{ud}}\Re_{\mathrm{HH},k_i}(\Delta u,0)$$
$$+\left(\rho_{\mathrm{H},k_i}^{\mathrm{ud}}\right)^2\Re_{\mathrm{HH},k_i}(0,0)+\sigma_{\mathrm{RS}}^2, \tag{C1}$$

where

$$\Re_{\mathrm{HH},k_i}(\Delta u,\Delta q)=E\left(H_{k_i,mn}^{uq}\left(H_{k_i,mn}^{(u+\Delta u)(q+\Delta q)}\right)^*\right).$$

We take the derivative of

$$E\left(\left|Y_{k_i,mn}^{uq}-\widehat{H}_{k_i,mn}^{uq}s_{k_i,m}^{uq}\right|^2\right)$$

$$\boldsymbol{B}_{k_i}=\left\{\left(\frac{\sigma_{\mathrm{G}}^2\xi_{\mathrm{G},k_i}^u}{\left(\xi_{\mathrm{G},k_i}^u\right)^2\rho_{\mathrm{G},k_i}^u\sigma_{\mathrm{G}}^2+\left(\rho_{\mathrm{G},k_i}^u\right)^3}-\frac{1}{\rho_{\mathrm{G},k_i}^u}\right)^2\left(\widehat{\boldsymbol{G}}_{k_i}^{(u-\Delta u)q}\right)^*\left(\widehat{\boldsymbol{G}}_{k_i}^{(u-\Delta u)q}\right)^{\mathrm{T}}\right.$$
$$\left.+\frac{N\sigma_{\mathrm{G}}^2\left(\xi_{\mathrm{G},k_i}^u\right)^2}{\left(\xi_{\mathrm{G},k_i}^u\right)^2\sigma_{\mathrm{G}}^2+\left(\rho_{\mathrm{G},k_i}^u\right)^2}\boldsymbol{I}_N\right\}\left\{\sigma_{\mathrm{RS}}^2\boldsymbol{I}_N+\frac{P_{\mathrm{RS}}}{N}\left[\left(\frac{\sigma_{\mathrm{G}}^2\xi_{\mathrm{G},k_{(-i)}}^u}{\left(\xi_{\mathrm{G},k_{(-i)}}^u\right)^2\rho_{\mathrm{G},k_{(-i)}}^u\sigma_{\mathrm{G}}^2+\left(\rho_{\mathrm{G},k_{(-i)}}^u\right)^3}\right.\right.$$
$$\left.-\frac{1-\rho_{\mathrm{G},k_{(-i)}}^u}{\rho_{\mathrm{G},k_{(-i)}}^u}\right)^2\left(\widehat{\boldsymbol{G}}_{k_{(-i)}}^{(u-\Delta u)q}\right)^*\left(\widehat{\boldsymbol{G}}_{k_{(-i)}}^{(u-\Delta u)q}\right)^{\mathrm{T}}+\frac{N\sigma_{\mathrm{H}}^2\left(\xi_{\mathrm{G},k_{(-i)}}^u\right)^2}{\left(\xi_{\mathrm{G},k_{(-i)}}^u\right)^2\sigma_{\mathrm{G}}^2+\left(\rho_{\mathrm{G},k_{(-i)}}^u\right)^2}\boldsymbol{I}_N$$
$$+\sum_{k'=1,k'\neq k}^{K}\sum_{i'\in\{a,b\}}\left(\frac{\sigma_{\mathrm{G}}^2\xi_{\mathrm{G},k'_{i'}}^u}{\left(\xi_{\mathrm{G},k'_{i'}}^u\right)^2\rho_{\mathrm{G},k'_{i'}}^u\sigma_{\mathrm{G}}^2+\left(\rho_{\mathrm{G},k'_{i'}}^u\right)^3}-\frac{1}{\rho_{\mathrm{G},k'_{i'}}^u}\right)^2\left(\widehat{\boldsymbol{G}}_{k'_{i'}}^{(u-\Delta u)q}\right)^*\left(\widehat{\boldsymbol{G}}_{k'_{i'}}^{(u-\Delta u)q}\right)^{\mathrm{T}}$$
$$\left.\left.+\sum_{k'=1,k'\neq k}^{K}\sum_{i'\in\{a,b\}}\frac{N\sigma_{\mathrm{G}}^2\left(\xi_{\mathrm{G},k'_{i'}}^u\right)^2}{\left(\xi_{\mathrm{G},k'_{i'}}^u\right)^2\sigma_{\mathrm{G}}^2+\left(\rho_{\mathrm{G},k'_{i'}}^u\right)^2}\boldsymbol{I}_N\right]\right\}^{-1}. \tag{B4}$$

with respect to $\rho_{\mathrm{H},k_i}^{u\mathrm{d}}$ and set it to zero, and then we have

$$\begin{aligned}&\frac{\mathrm{d}E\left(\left|\tilde{Y}_{k_i,mn}^{uq}-\widehat{H}_{k_i,mn}^{uq}\tilde{s}_{k_i,m}^{uq}\right|^2\right)}{\mathrm{d}\rho_{\mathrm{H},k_i}^{u\mathrm{d}}}\\&=-2\Re_{\mathrm{HH},k_i}(\Delta u,0)+2\Re_{\mathrm{HH},k_i}(0,0)\rho_{\mathrm{H},k_i}^{u\mathrm{d}}\\&=0,\end{aligned} \tag{C2}$$

which gives

$$\rho_{\mathrm{H},k_i}^{u\mathrm{d}}=\frac{\Re_{\mathrm{HH},k_i}(\Delta u,0)}{\Re_{\mathrm{HH},k_i}(0,0)}, \tag{C3}$$

which is the error coefficient from the time-variant property of the channel.

Appendix D: Derivation of $\rho_{\mathrm{H},k_i}^{u\mathrm{e}}$

In what follows, when the MMSE-based channel estimator is used, the estimated channel complex gain is given by the form

$$\widehat{H}_{k_i,mn}^{(u-\Delta u)q}=\frac{\mathrm{SNR}_{\mathrm{H},k_i}^{u\mathrm{p}}}{1+\mathrm{SNR}_{\mathrm{H},k_i}^{u\mathrm{p}}}H_{k_i,mn}^{uq}+\frac{E\left[H_{k_i,mn}^{uq}\left(H_{k_i,mn}^{uq}\right)^*\left(\tilde{s}_{k_i,m}^{uq}\right)^*\right]\tilde{z}_{k_i,n}^{uq}}{E\left[H_{k_i,mn}^{uq}\left(H_{k_i,mn}^{uq}\right)^*\left(\tilde{s}_{k_i,m}^{uq}\right)^*\left(\tilde{s}_{k_i,m}^{uq}\right)+\sigma_{\mathrm{RS}}^2\right]}, \tag{D1}$$

where

$$\mathrm{SNR}_{\mathrm{H},k_i}^{u\mathrm{p}}=\frac{E\left[H_{k_i,mn}^{uq}\left(H_{k_i,mn}^{uq}\right)^*\left(\tilde{s}_{k_i,m}^{uq}\right)^*\tilde{s}_{k_i,m}^{uq}\right]}{\sigma_{\mathrm{RS}}^2}$$

is the equivalent SNR at pilot grids which can be estimated by the average SNR at data grids in terms of the relation that between them as shown in Eq. (34). From the first term in the right-hand side of Eq. (D1), it is obvious

$$\rho_{\mathrm{H},k_i}^{u\mathrm{e}}=\frac{\mathrm{SNR}_{\mathrm{H},k_i}^{u\mathrm{p}}}{1+\mathrm{SNR}_{\mathrm{H},k_i}^{u\mathrm{p}}}, \tag{D2}$$

which is the error coefficient produced by channel estimation.

Appendix E: CP-based estimation of SNR

In accordance with Ijaz *et al.* (2011), the average power of the uth received pilot OFDM symbols at the mth antenna of user k_i is equal to the sum of signal and noise power

$$\begin{aligned}&\frac{1}{2L}\left(\sum_{t=0}^{L-1}\left|\bar{y}_{k_i,mn}^u(t)\right|^2+\sum_{t=N_{\mathrm{C}}}^{N_{\mathrm{C}}+L-1}\left|\bar{y}_{k_i,mn}^u(t)\right|^2\right)\\&\approx\widehat{P}_{S,k_i,mn}^u+\widehat{P}_{N,k_i,mn}^u,\end{aligned} \tag{E1}$$

where $\widehat{P}_{S,k_i,mn}$ denotes the average power of useful data signal at the receive signal, and $\widehat{P}_{N,k_i,mn}$ is the average power of AWGN noise in the channel.

Making use of the cyclic property of CP of the OFDM symbol, the correlation function between CP and its corresponding part in the OFDM symbol is approximated to be the average useful symbol power:

$$\widehat{P}^u_{S,k_i,mn} = \frac{1}{LN_{\mathrm{p}}} \sum_{u=1}^{N_{\mathrm{p}}} \sum_{t=0}^{L-1} \left| \bar{y}^u_{k_i,mn}(t) \left(\bar{y}^u_{k_i,mn}(t+N_{\mathrm{C}}) \right)^* \right| \quad \text{(E2)}$$

due to the independent property of noise. Substituting Eq. (E2) into Eq. (E1) yields

$$\widehat{P}^u_{N,k_i,mn} = \frac{1}{2LN_{\mathrm{p}}} \sum_{u=1}^{N_{\mathrm{p}}} \left(\sum_{t=0}^{L-1} \left(\left| \bar{y}^u_{k_i,mn}(t) \right| - \left| \bar{y}^u_{k_i,mn}(t+N_{\mathrm{C}}) \right| \right)^2 \right). \quad \text{(E3)}$$

Combining Eqs. (E2) and (E3) forms the estimated average SNR at data grids:

$$\mathrm{SNR}^{u\mathrm{d}}_{\mathrm{H},k_i} = \frac{\sum_{m=1}^{M} \sum_{n=1}^{N} \widehat{P}^u_{S,k_i,mn}}{\sum_{m=1}^{M} \sum_{n=1}^{N} \widehat{P}^u_{N,k_i,mn}} = \frac{\sum_{u=1}^{N_{\mathrm{p}}} \sum_{m=1}^{M} \sum_{n=1}^{N} \sum_{t=0}^{L-1} \left| \bar{y}^u_{k_i,mn}(t) \left(\bar{y}^u_{k_i,mn}(t+N_{\mathrm{C}}) \right)^* \right|}{2 \sum_{u=1}^{N_{\mathrm{p}}} \sum_{m=1}^{M} \sum_{n=1}^{N} \sum_{t=0}^{L-1} \left(\left| \bar{y}^u_{k_i,mn}(t) \right| - \left| \bar{y}^u_{k_i,mn}(t+N_{\mathrm{C}}) \right| \right)^2}. \quad \text{(E4)}$$